

Gravitational Wave Astrophysics

Pablo Marchant

Outline

Today

12/5

19/5

- History of the field
- Types of detectors
- Types of sources
- Current state of the field
- Future advancements
- Ground based interferometers
- Production of GWs from compact object binaries
- Parameter estimation from observed compact object coalescences
- Astrophysics of observed GW sources

Outline

Today

- History of the field
- Types of detectors
- Types of sources
- Current state of the field
- Future advancements

12/5

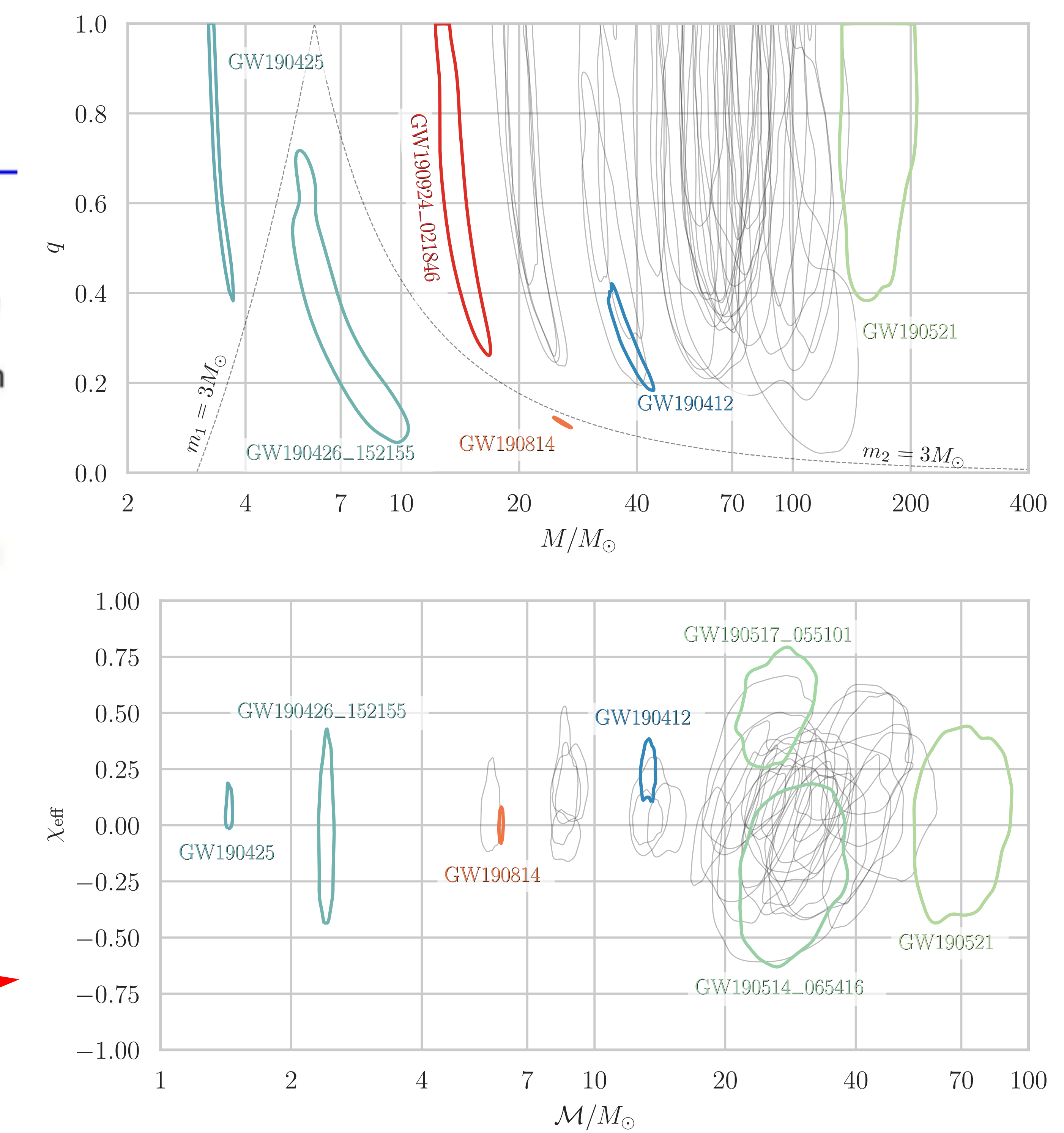
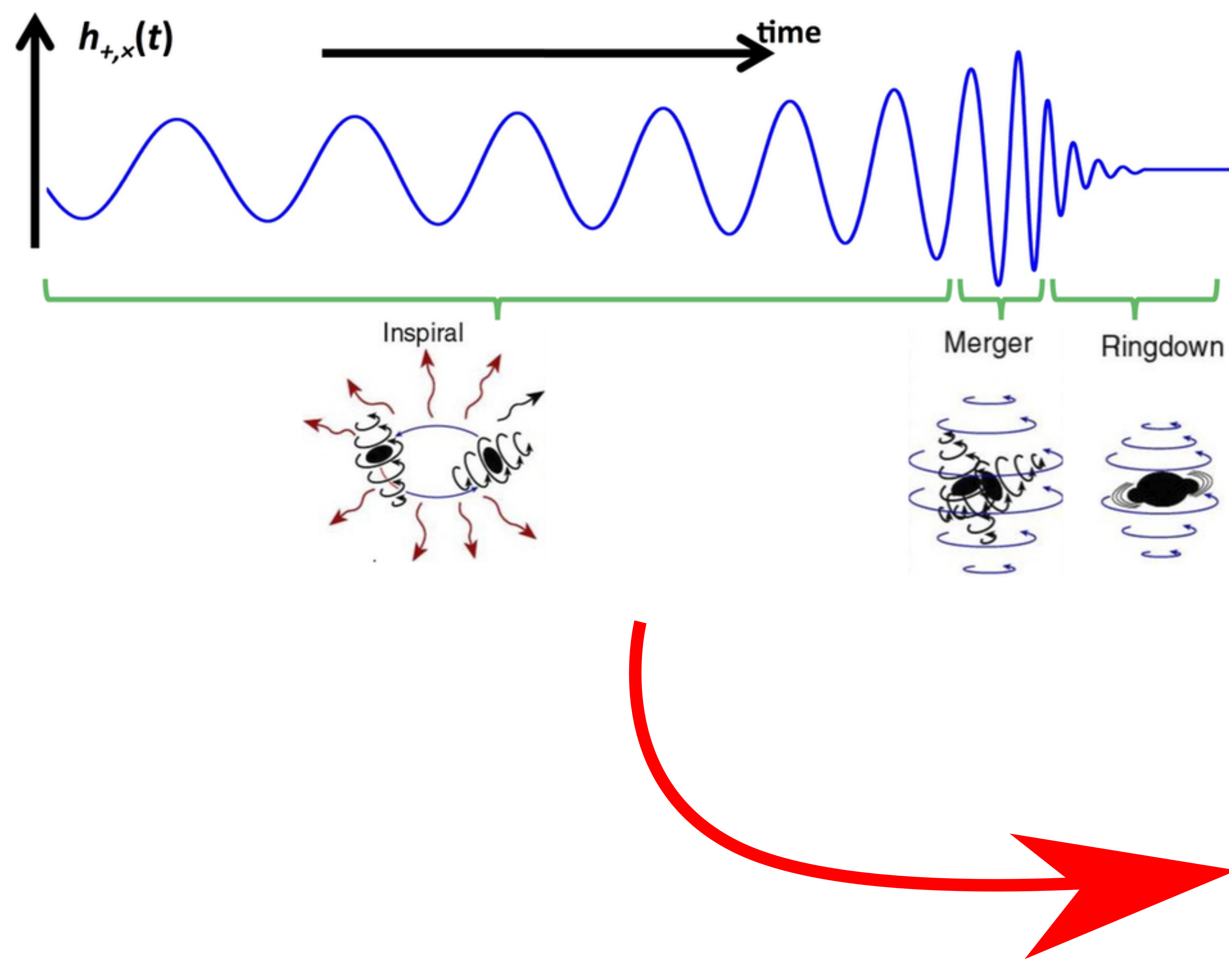
- Ground based interferometers
- Production of GWs from compact object binaries

19/5

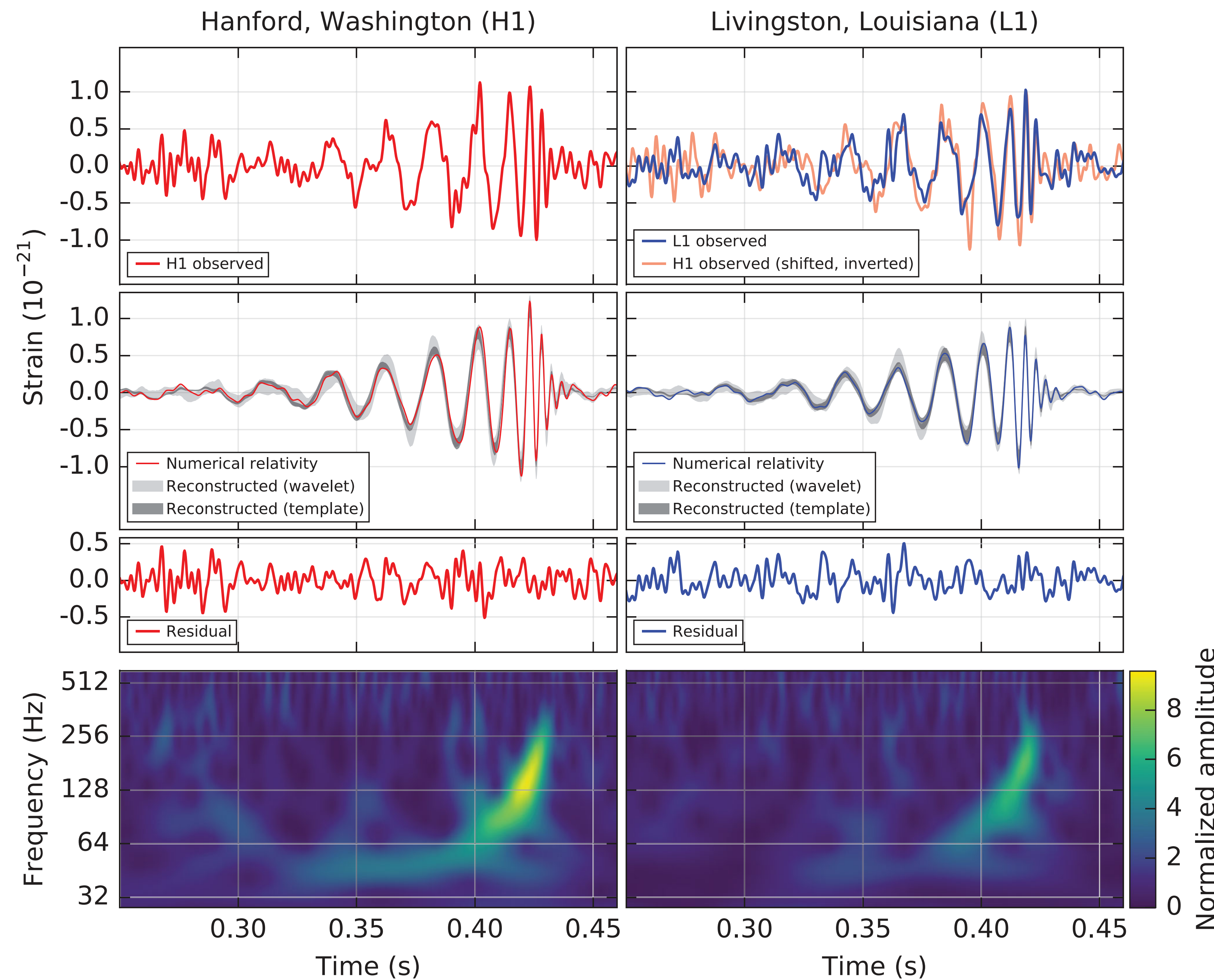
- Parameter estimation from observed compact object coalescences
- Astrophysics of observed GW sources

From data to binary properties

How do we move from an observed waveform to a set of properties in a compact binary coalescence?

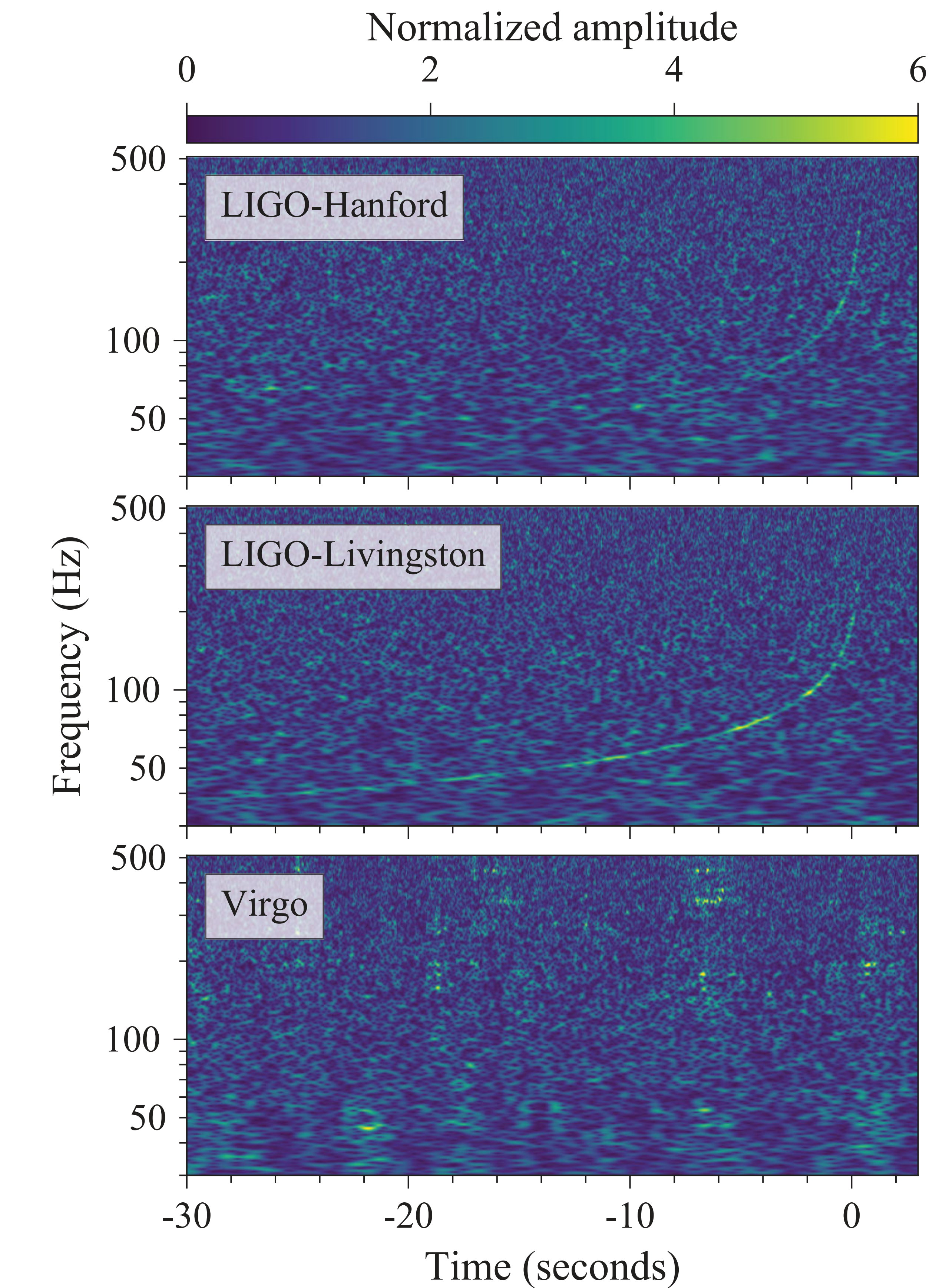
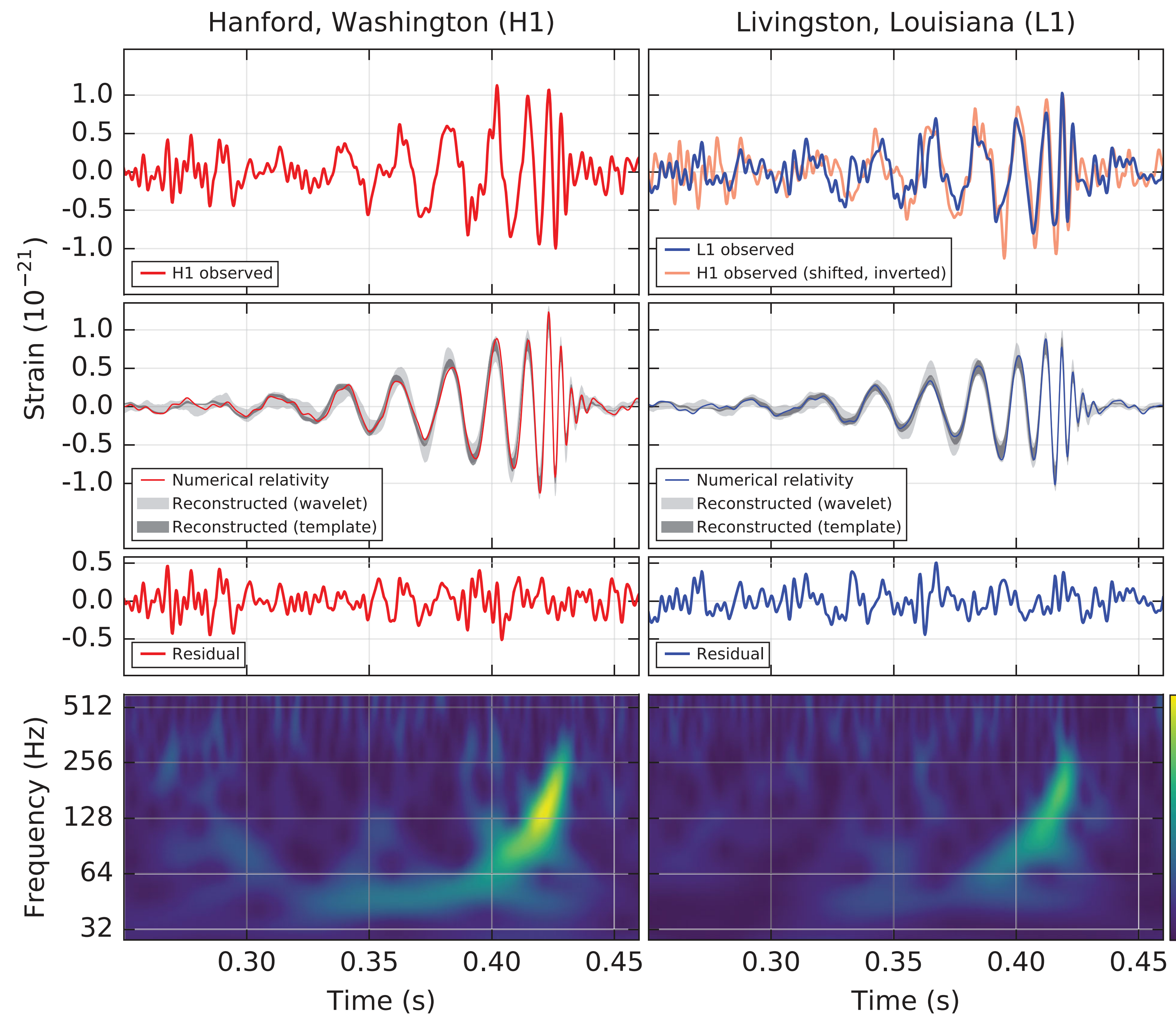


Detectors are noisy!



GW150914, discovery paper
Physical Review Letters 116, 061102 (2016)

Detectors are noisy!

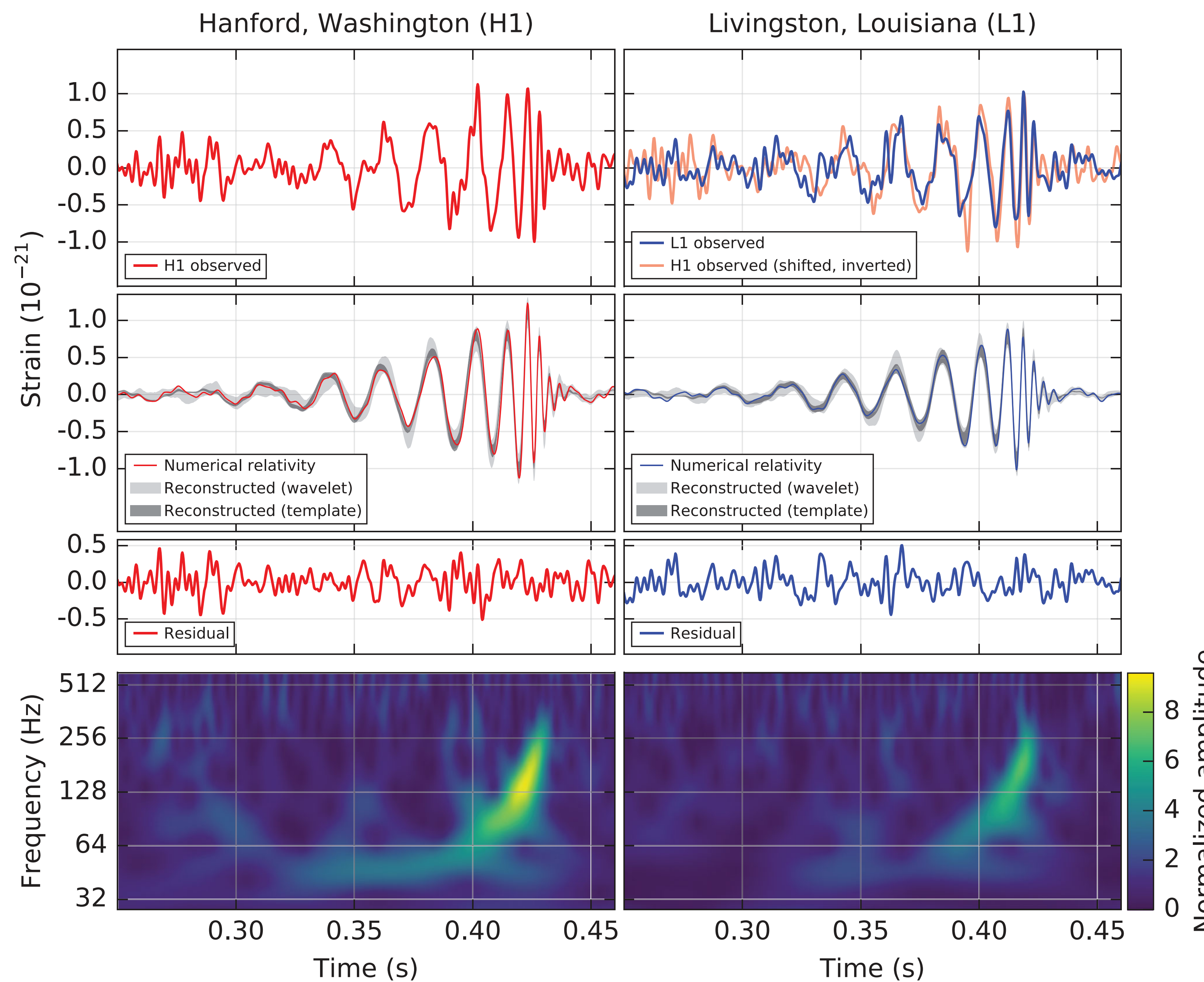


GW150914, discovery paper

Physical Review Letters 116, 061102 (2016)

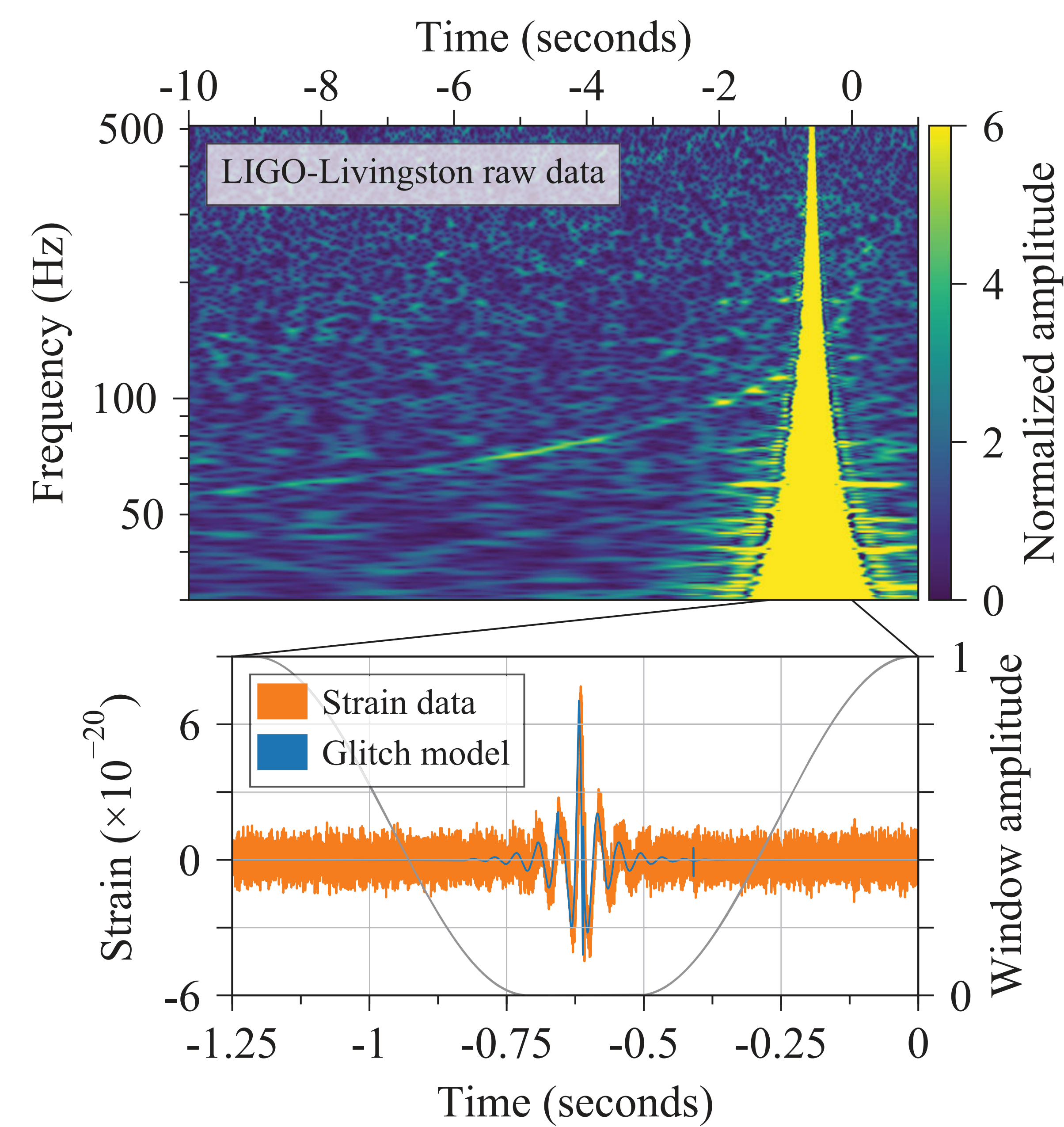
GW170817 (binary NS), discovery paper
Physical Review Letters 119, 161101 (2017)

Detectors are noisy!



GW150914, discovery paper
Physical Review Letters 116, 061102 (2016)

Actual data for GW170817 showed a very strong glitch in LIGO-Livingston!
Rapidly cleaning this signal was an important part on the effort to find its EM counterpart.



GW170817 (binary NS), discovery paper
Physical Review Letters 119, 161101 (2017)

Detectors are noisy!

Signal in an interferometer will always be a combination of an actual GW signal and the interferometer noise.

$$s(t) = n(t) + h(t)$$

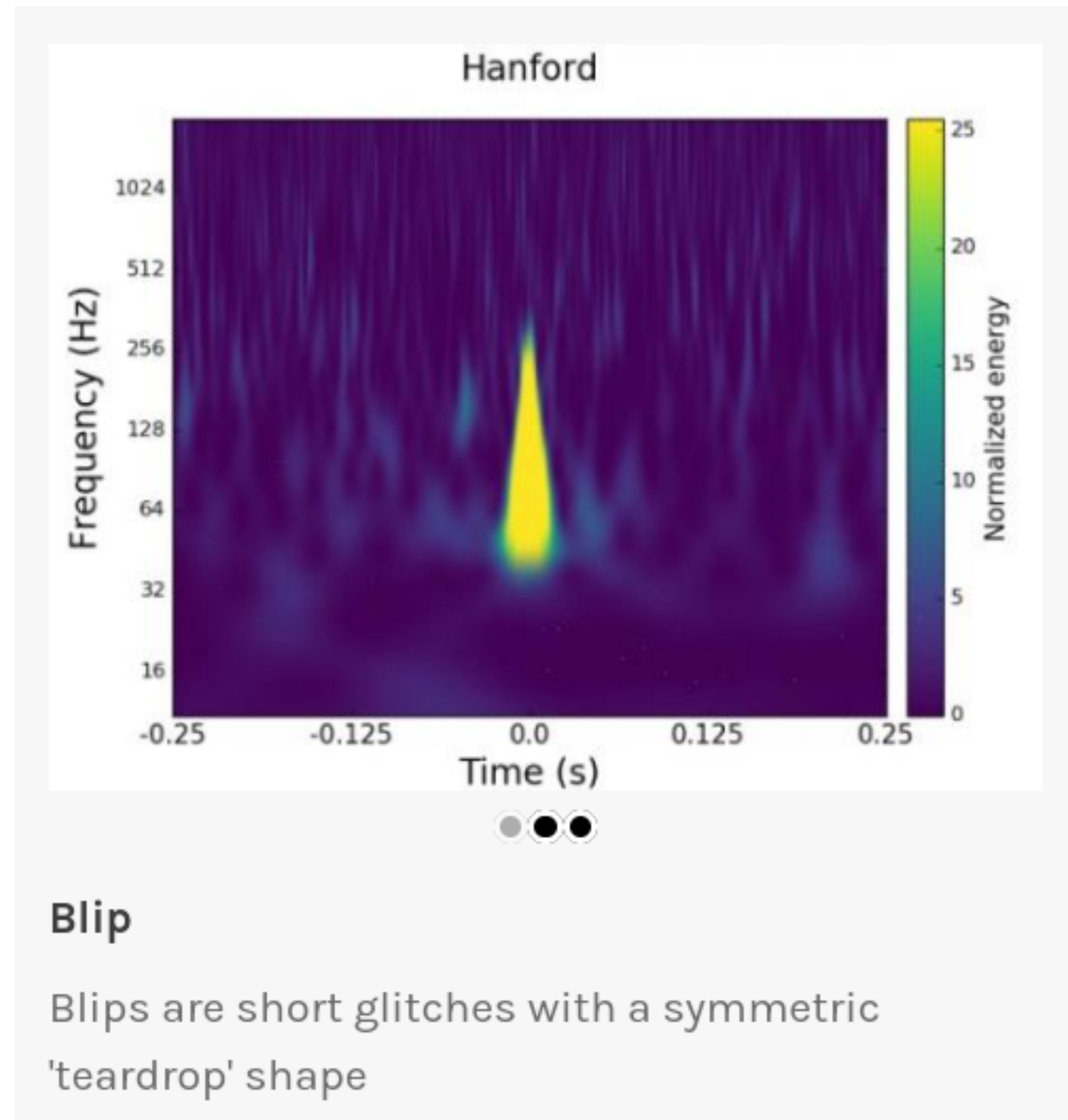
Sudden events of noise in the detector can be interpreted as fake signals. There is a significant effort to characterize not just the steady well behaved noise spectrum but also these "glitches"

Detectors are noisy!

Signal in an interferometer will always be a combination of an actual GW signal and the interferometer noise.

$$s(t) = n(t) + h(t)$$

Sudden events of noise in the detector can be interpreted as fake signals. There is a significant effort to characterize not just the steady well behaved noise spectrum but also these "glitches"



One example of a common glitch in LIGO data

<https://www.zooniverse.org/projects/zooniverse/gravity-spy>

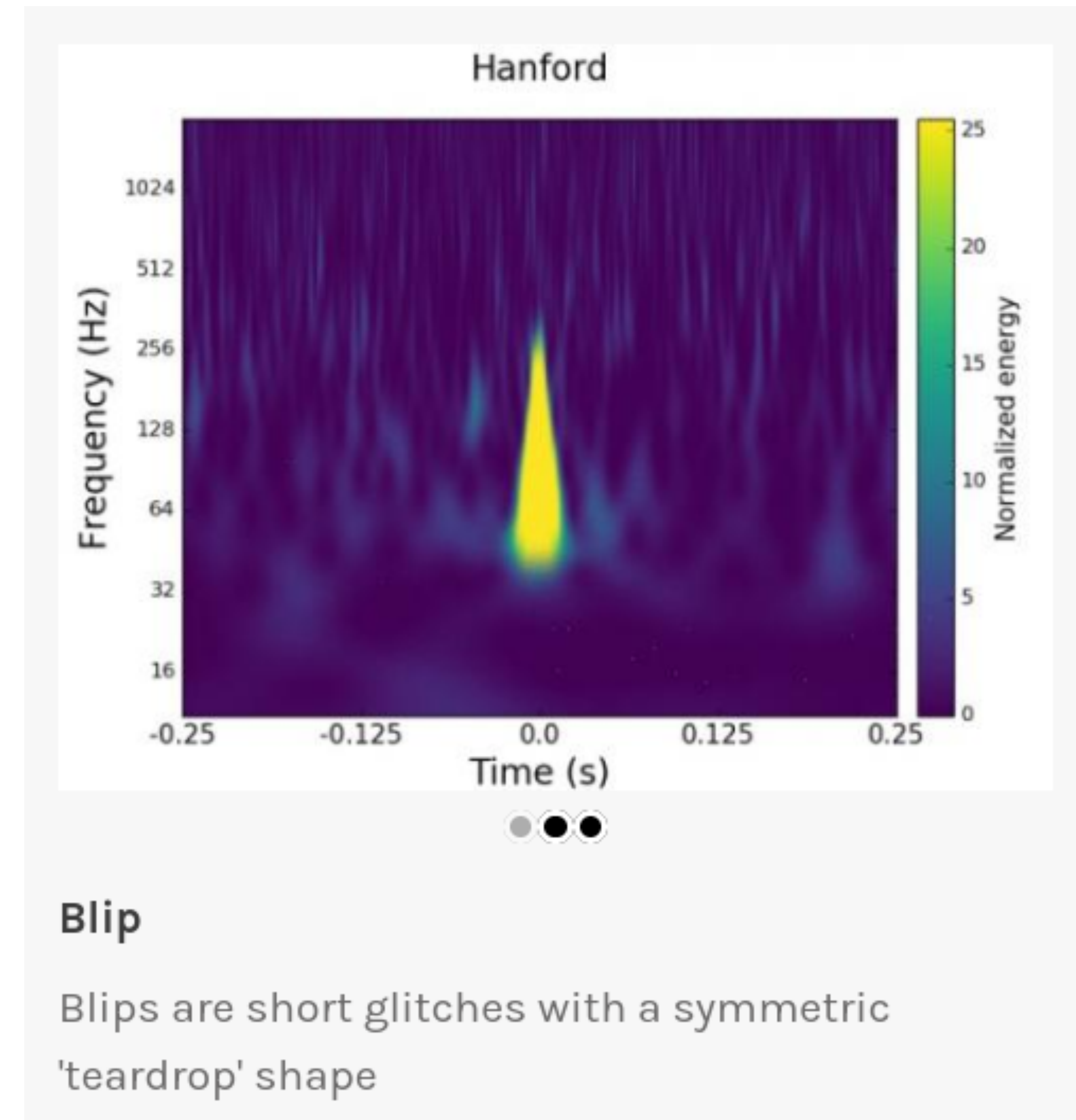
Detectors are noisy!

Signal in an interferometer will always be a combination of an actual GW signal and the interferometer noise.

$$s(t) = n(t) + h(t)$$

Sudden events of noise in the detector can be interpreted as fake signals. There is a significant effort to characterize not just the steady well behaved noise spectrum but also these "glitches"

Network of interferometers is critical to distinguish real from artificial signals!



One example of a common glitch in LIGO data
<https://www.zooniverse.org/projects/zooniverse/gravity-spy>

Matched filtering

For each template $h(t)$ and for the strain data from a single detector $s(t)$, the analysis calculates the square of the matched-filter SNR defined by [12]

$$\rho^2(t) \equiv \frac{1}{\langle h|h \rangle} |\langle s|h \rangle(t)|^2, \quad (1)$$

where the correlation is defined by

$$\langle s|h \rangle(t) = 4 \int_0^\infty \frac{\tilde{s}(f)\tilde{h}^*(f)}{S_n(f)} e^{2\pi ift} df, \quad (2)$$

where $\tilde{s}(f)$ is the Fourier transform of the time domain quantity $s(t)$ given by

$$\tilde{s}(f) = \int_{-\infty}^\infty s(t)e^{-2\pi ift} dt. \quad (3)$$

The quantity $S_n(|f|)$ is the one-sided average power spectral density of the detector noise, which is re-calculated every 2048 s (in contrast to the fixed spectrum used in template bank construction). Calculation of the matched-filter SNR in the frequency domain allows the use of the computationally efficient Fast Fourier Transform [80, 81]. The square of the matched-filter SNR in Eq. (1) is normalized by

$$\langle h|h \rangle = 4 \int_0^\infty \frac{\tilde{h}(f)\tilde{h}^*(f)}{S_n(f)} df, \quad (4)$$

so that its mean value is 2, if $s(t)$ contains only stationary noise [82].

CBC stands for compact binary coalescence. In this case we know from first principles what a signal should look like and we can search through the data for it. The method used for this is called **matched filtering**.

Matched filtering

For each template $h(t)$ and for the strain data from a single detector $s(t)$, the analysis calculates the square of the matched-filter SNR defined by [12]

$$\rho^2(t) \equiv \frac{1}{\langle h|h \rangle} |\langle s|h \rangle(t)|^2, \quad (1)$$

where the correlation is defined by

$$\langle s|h \rangle(t) = 4 \int_0^\infty \frac{\tilde{s}(f)\tilde{h}^*(f)}{S_n(f)} e^{2\pi ift} df, \quad (2)$$

where $\tilde{s}(f)$ is the Fourier transform of the time domain quantity $s(t)$ given by

$$\tilde{s}(f) = \int_{-\infty}^\infty s(t)e^{-2\pi ift} dt. \quad (3)$$

The quantity $S_n(|f|)$ is the one-sided average power spectral density of the detector noise, which is re-calculated every 2048 s (in contrast to the fixed spectrum used in template bank construction). Calculation of the matched-filter SNR in the frequency domain allows the use of the computationally efficient Fast Fourier Transform [80, 81]. The square of the matched-filter SNR in Eq. (1) is normalized by

$$\langle h|h \rangle = 4 \int_0^\infty \frac{\tilde{h}(f)\tilde{h}^*(f)}{S_n(f)} df, \quad (4)$$

so that its mean value is 2, if $s(t)$ contains only stationary noise [82].

CBC stands for compact binary coalescence. In this case we know from first principles what a signal should look like and we can search through the data for it. The method used for this is called **matched filtering**.

Signal is further weighted by additional criteria that checks for the resemblance of a signal to a CBC,

$$\hat{\rho} = \begin{cases} \rho / [(1 + (\chi_r^2)^3)/2]^{1/6}, & \text{if } \chi_r^2 > 1, \\ \rho, & \text{if } \chi_r^2 \leq 1. \end{cases}$$

Matched filtering

For each template $h(t)$ and for the strain data from a single detector $s(t)$, the analysis calculates the square of the matched-filter SNR defined by [12]

$$\rho^2(t) \equiv \frac{1}{\langle h|h \rangle} |\langle s|h \rangle(t)|^2, \quad (1)$$

where the correlation is defined by

$$\langle s|h \rangle(t) = 4 \int_0^\infty \frac{\tilde{s}(f)\tilde{h}^*(f)}{S_n(f)} e^{2\pi ift} df, \quad (2)$$

where $\tilde{s}(f)$ is the Fourier transform of the time domain quantity $s(t)$ given by

$$\tilde{s}(f) = \int_{-\infty}^\infty s(t)e^{-2\pi ift} dt. \quad (3)$$

The quantity $S_n(|f|)$ is the one-sided average power spectral density of the detector noise, which is re-calculated every 2048 s (in contrast to the fixed spectrum used in template bank construction). Calculation of the matched-filter SNR in the frequency domain allows the use of the computationally efficient Fast Fourier Transform [80, 81]. The square of the matched-filter SNR in Eq. (1) is normalized by

$$\langle h|h \rangle = 4 \int_0^\infty \frac{\tilde{h}(f)\tilde{h}^*(f)}{S_n(f)} df, \quad (4)$$

so that its mean value is 2, if $s(t)$ contains only stationary noise [82].

GW150914, CBC search paper
Phys. Rev. D 93, 122003 (2016)

CBC stands for compact binary coalescence. In this case we know from first principles what a signal should look like and we can search through the data for it. The method used for this is called **matched filtering**.

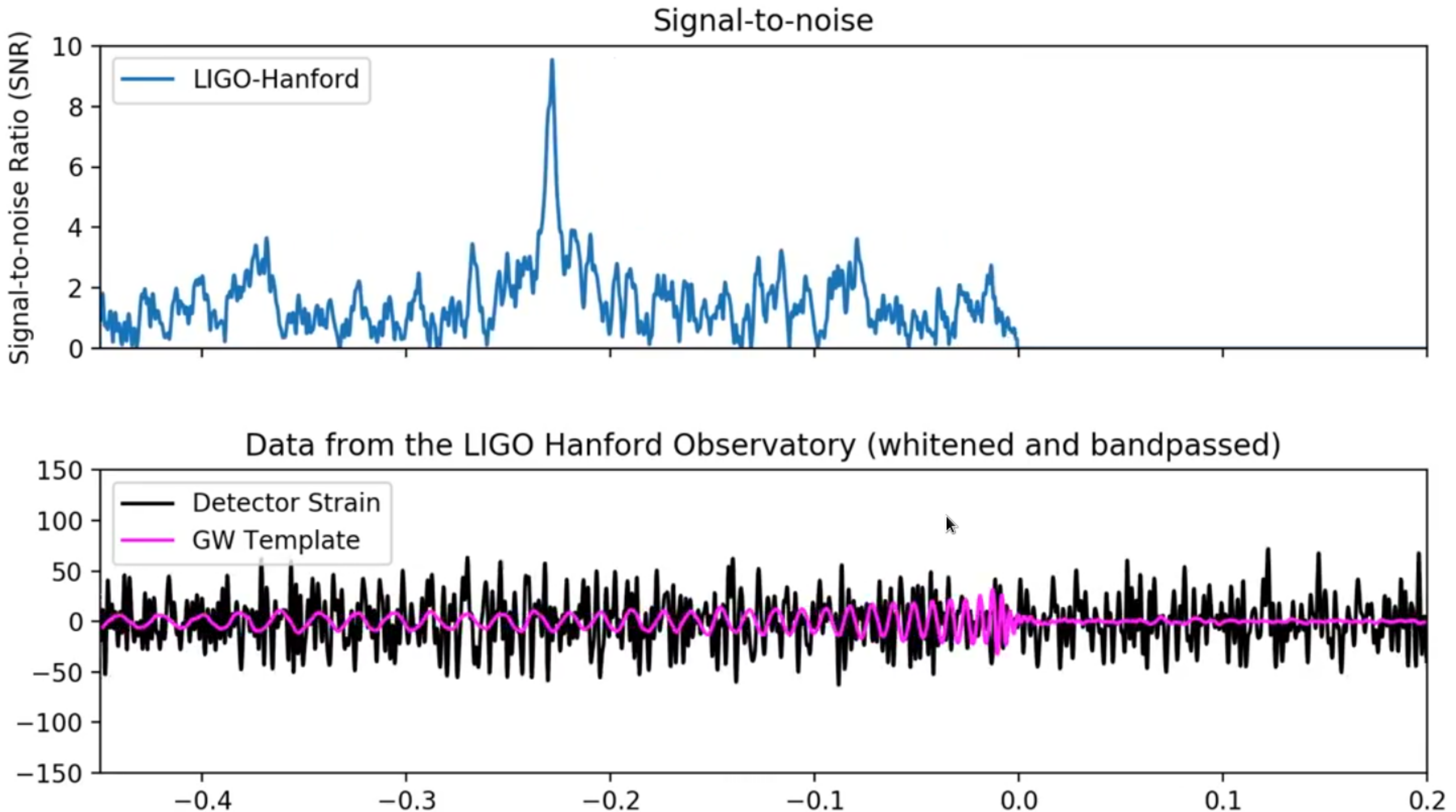
Signal is further weighted by additional criteria that checks for the resemblance of a signal to a CBC,

$$\hat{\rho} = \begin{cases} \rho / [(1 + (\chi_r^2)^3)/2]^{1/6}, & \text{if } \chi_r^2 > 1, \\ \rho, & \text{if } \chi_r^2 \leq 1. \end{cases}$$

A final "detection statistic" is built by averaging the weighted SNR between detectors. For two LIGO detectors this is:

$$\hat{\rho}_c = \sqrt{\hat{\rho}_{c,\text{Hanford}} + \hat{\rho}_{c,\text{Livingston}}}$$

Matched filtering



Matched filtering for GW151226 (binary BH merger). Credit: A. Nitz
<https://www.youtube.com/watch?v=bBBDR5jf9oU>

Matched filtering

Signal-to-noise Ratio (SNR)

Exercise 1

Let's make a simple illustration of how matched filtering does this shift in time to compare to a template. Imagine a "signal" and a "template" given by:

$$s(t) = f(t - t_0), \quad h(t) = f(t)$$

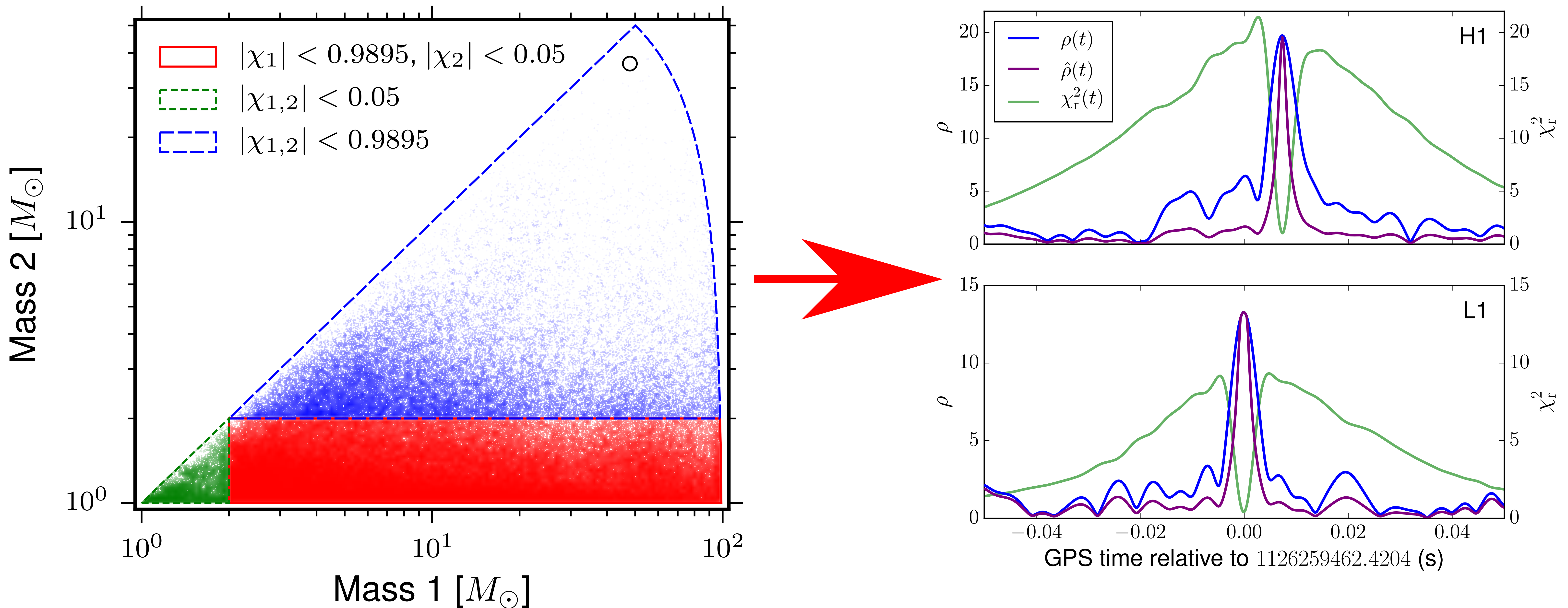
The template is just the same as the signal but shifted in time. What value of t gives the maximum for the following integral?

$$\int_0^\infty \tilde{s}(f) \tilde{h}^*(f) e^{2\pi i f t} df$$

<https://www.youtube.com/watch?v=bBBDR5jf9oU>

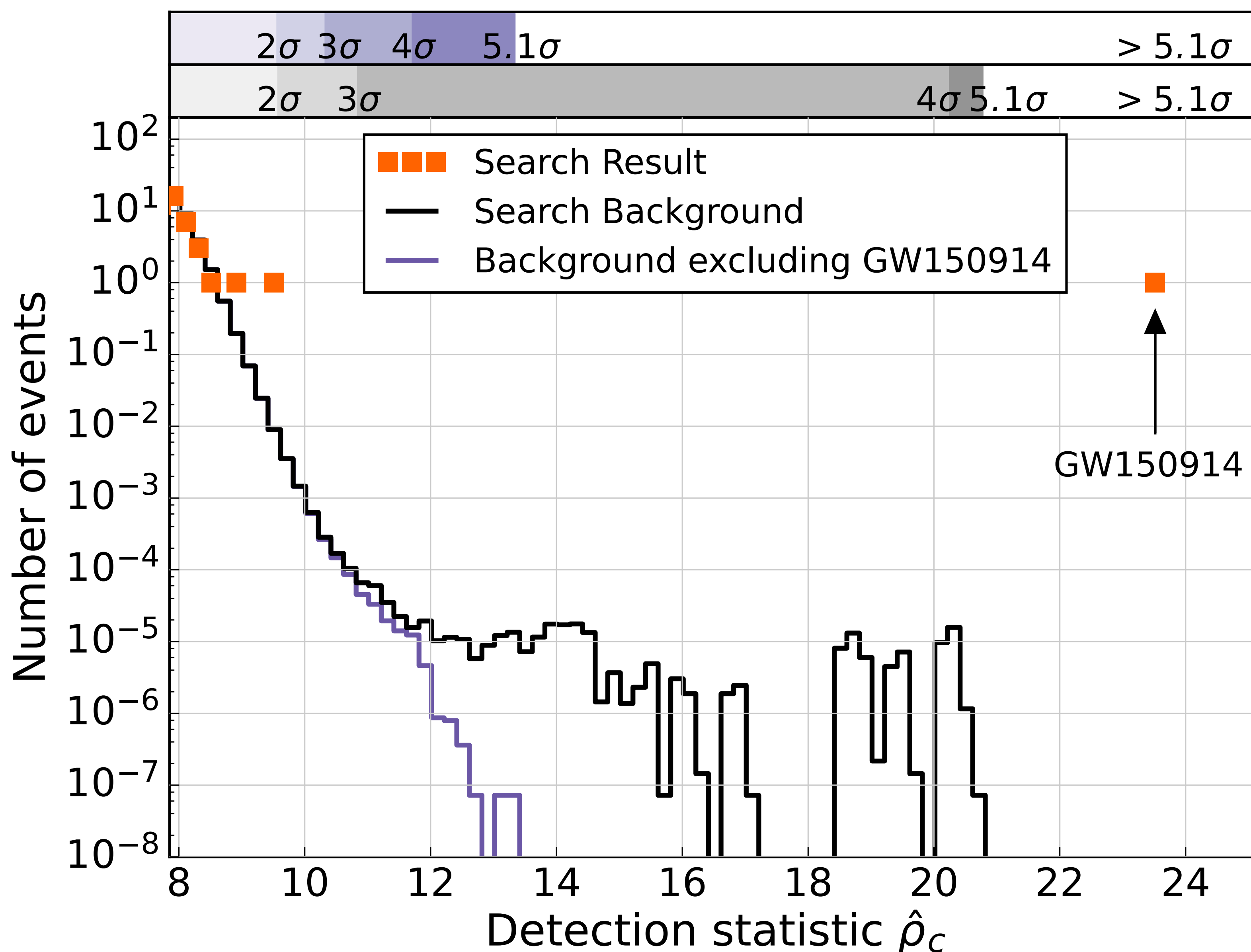
Matched filtering (GW150914)

GW150914, CBC search paper, Phys. Rev. D 93, 122003 (2016)



Applying matched filtering from a template bank
to the data yields one template with a high
detection statistic. **Is this a spurious result?**

Matched filtering (GW150914)



The rate of high significance events can be determined from the data itself. With a network of detectors, artificially long stretches of data can be produced by **time-shifting** them with respect to each other.

Time-shifting produces artificial high significance events when the signal of GW150914 matches a glitch.

This analysis provides a measure of the **false-alarm rate** of a detection.

GW150914, CBC search paper,
Phys. Rev. D 93, 122003 (2016)

Matched filtering (GW150914)

GWTC-1: A GRAVITATIONAL-WAVE TRANSIENT CATALOG ...

PHYS. REV. X **9**, 031040 (2019)

TABLE I. Search results for the 11 GW events. We report a false-alarm rate for each search that found a given event; otherwise, we display \dots . The network SNR for the two matched-filter searches is that of the template ranked highest by that search, which is not necessarily the template with the highest SNR. Moreover, the network SNR is the quadrature sum of the detectors coincident in the highest-ranked trigger; in some cases, only two detectors contribute, even if all three are operating nominally at the time of that event.

Event	UTC time	FAR [y^{-1}]			Network SNR		
		PyCBC	GstLAL	cWB	PyCBC	GstLAL	cWB
GW150914	09:50:45.4	$<1.53 \times 10^{-5}$	$<1.00 \times 10^{-7}$	$<1.63 \times 10^{-4}$	23.6	24.4	25.2
GW151012	09:54:43.4	0.17	7.92×10^{-3}	\dots	9.5	10.0	\dots
GW151226	03:38:53.6	$<1.69 \times 10^{-5}$	$<1.00 \times 10^{-7}$	0.02	13.1	13.1	11.9
GW170104	10:11:58.6	$<1.37 \times 10^{-5}$	$<1.00 \times 10^{-7}$	2.91×10^{-4}	13.0	13.0	13.0
GW170608	02:01:16.5	$<3.09 \times 10^{-4}$	$<1.00 \times 10^{-7}$	1.44×10^{-4}	15.4	14.9	14.1
GW170729	18:56:29.3	1.36	0.18	0.02	9.8	10.8	10.2
GW170809	08:28:21.8	1.45×10^{-4}	$<1.00 \times 10^{-7}$	\dots	12.2	12.4	\dots
GW170814	10:30:43.5	$<1.25 \times 10^{-5}$	$<1.00 \times 10^{-7}$	$<2.08 \times 10^{-4}$	16.3	15.9	17.2
GW170817	12:41:04.4	$<1.25 \times 10^{-5}$	$<1.00 \times 10^{-7}$	\dots	30.9	33.0	\dots
GW170818	02:25:09.1	\dots	4.20×10^{-5}	\dots	\dots	11.3	\dots
GW170823	13:13:58.5	$<3.29 \times 10^{-5}$	$<1.00 \times 10^{-7}$	2.14×10^{-3}	11.1	11.5	10.8

Inferring source parameters

After identifying a signal, what information can be extracted from it?

Inferring source parameters

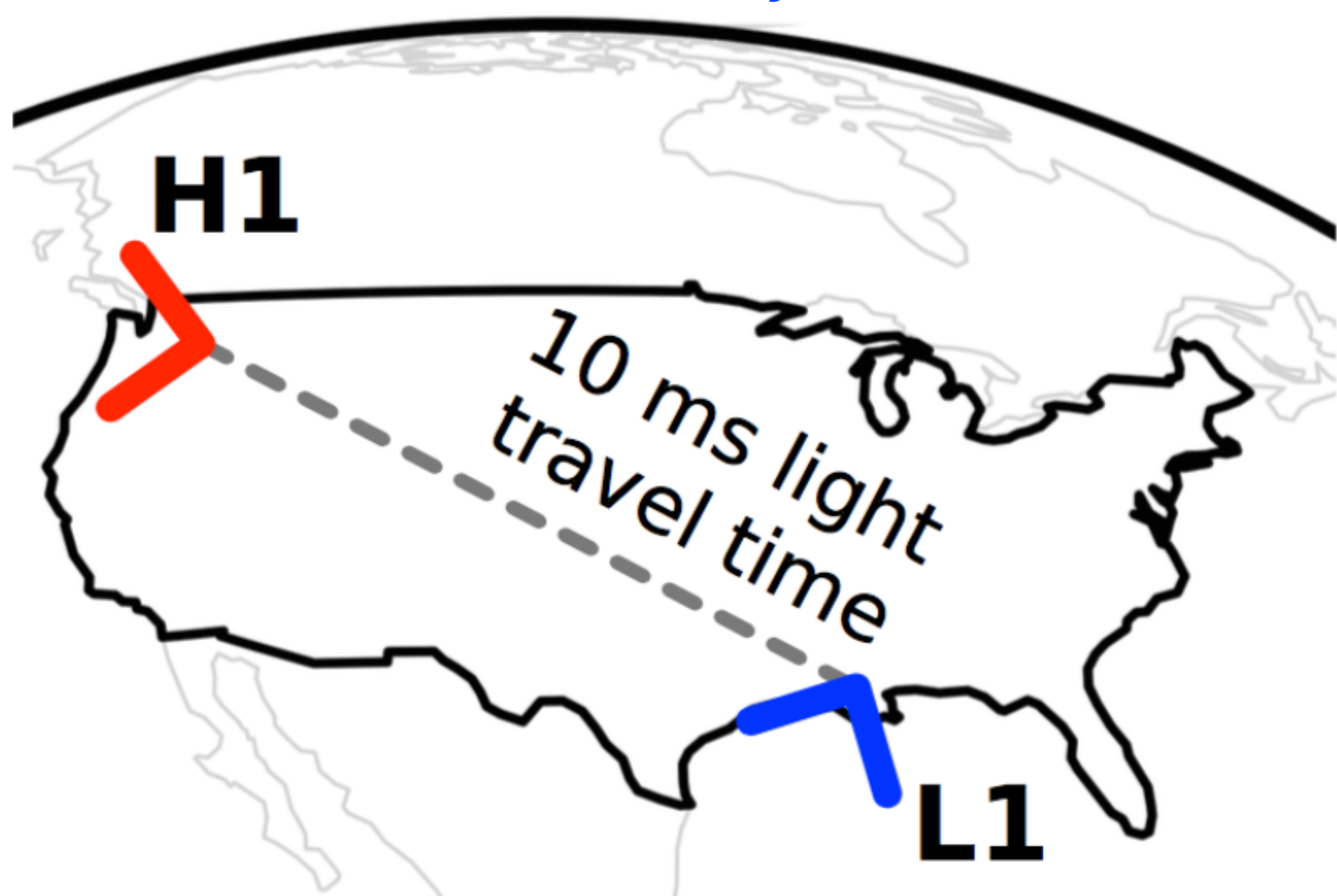
After identifying a signal, what information can be extracted from it?

Intrinsic parameters:

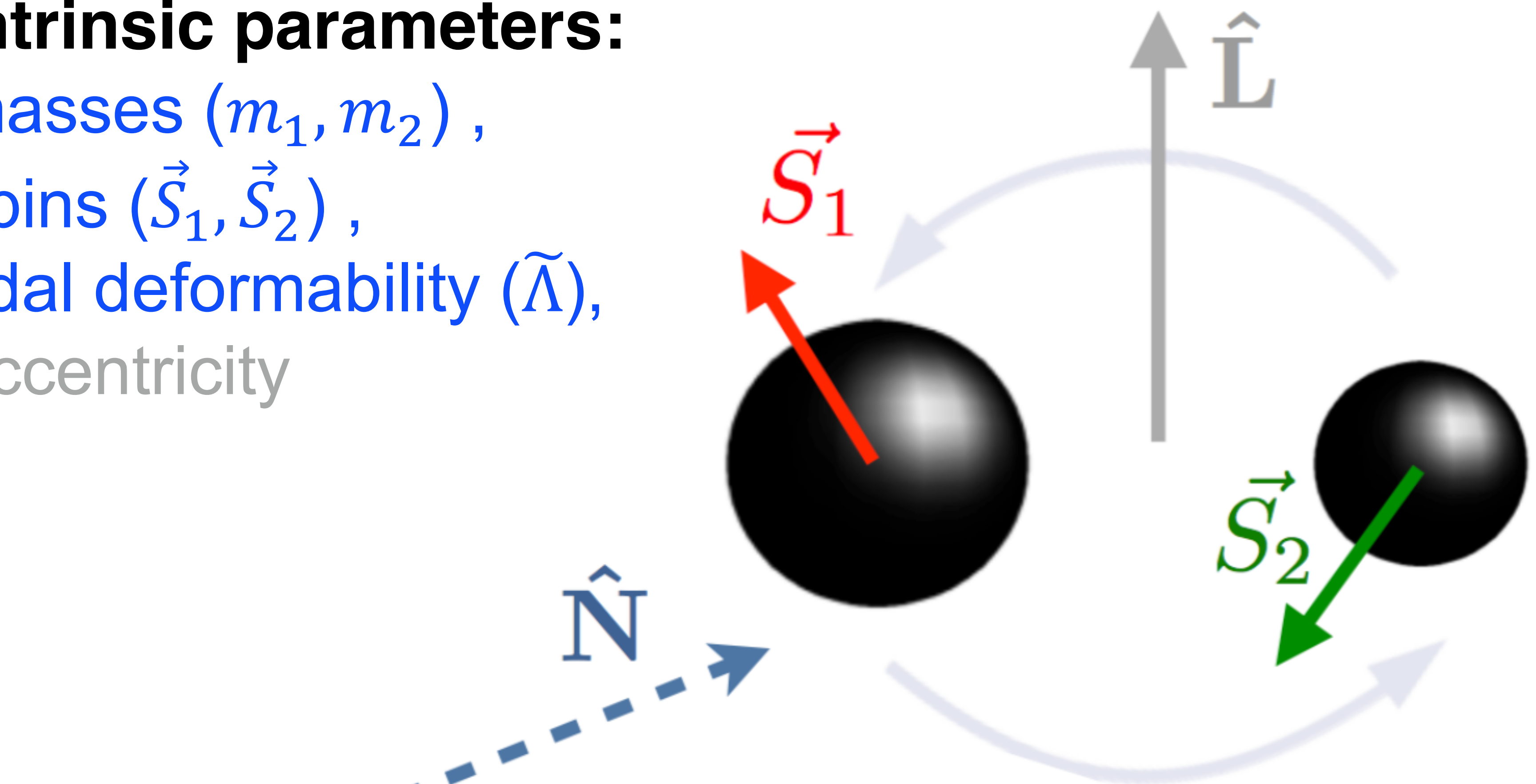
masses (m_1, m_2),
spins (\vec{S}_1, \vec{S}_2),
tidal deformability ($\tilde{\Lambda}$),
eccentricity

Extrinsic parameters:

time (t_c), reference phase (φ_c),
sky position (α, δ), distance (d_L),
orbital orientation (θ_{Jn}, ψ),



Credit: LIGO/Virgo



Spin magnitudes and orientations, eccentricity, ... tell us something about how these binaries formed

Credit: Alan J. Weinstein

Inferring source parameters

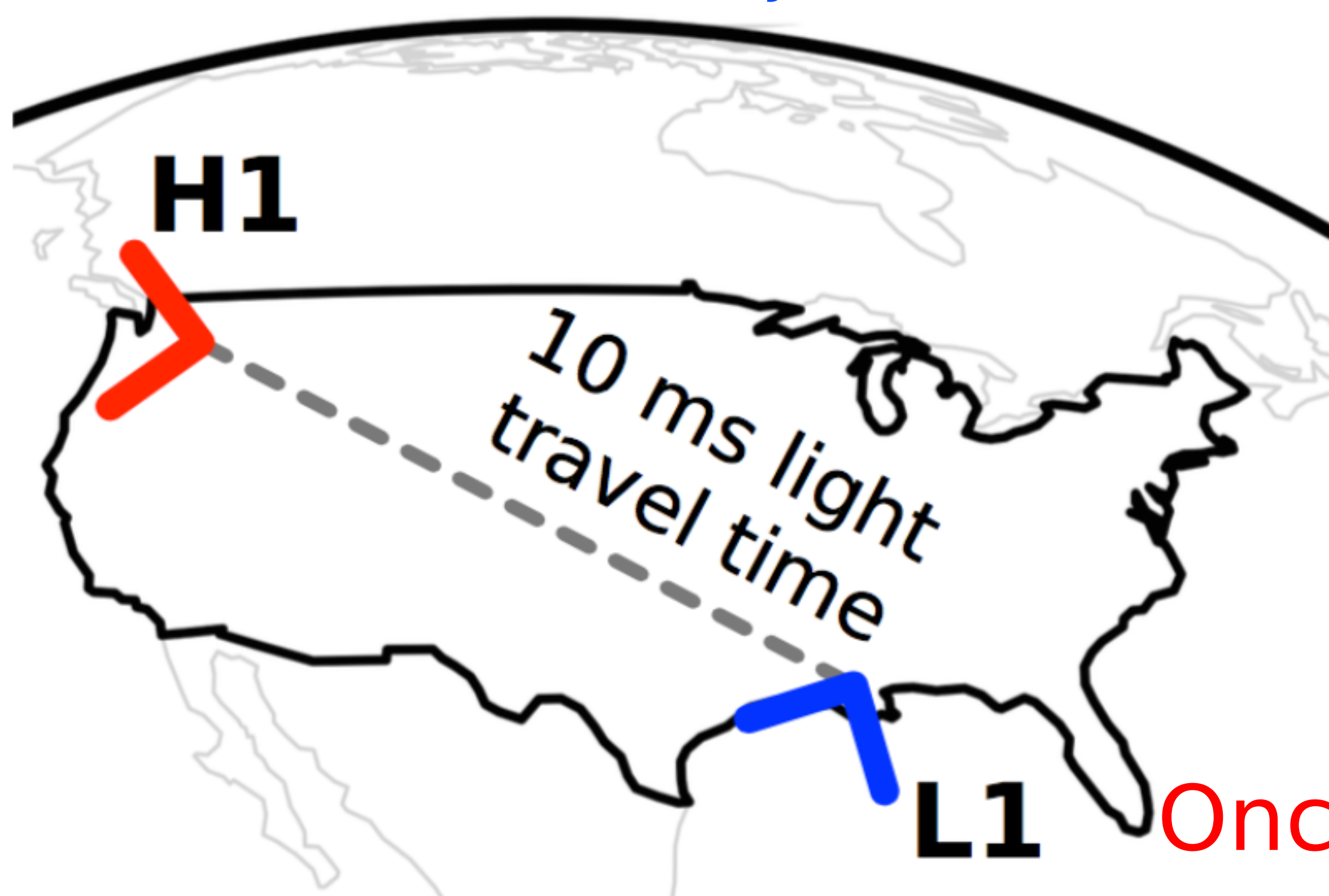
After identifying a signal, what information can be extracted from it?

Intrinsic parameters:

masses (m_1, m_2),
spins (\vec{S}_1, \vec{S}_2),
tidal deformability ($\tilde{\Lambda}$),
eccentricity

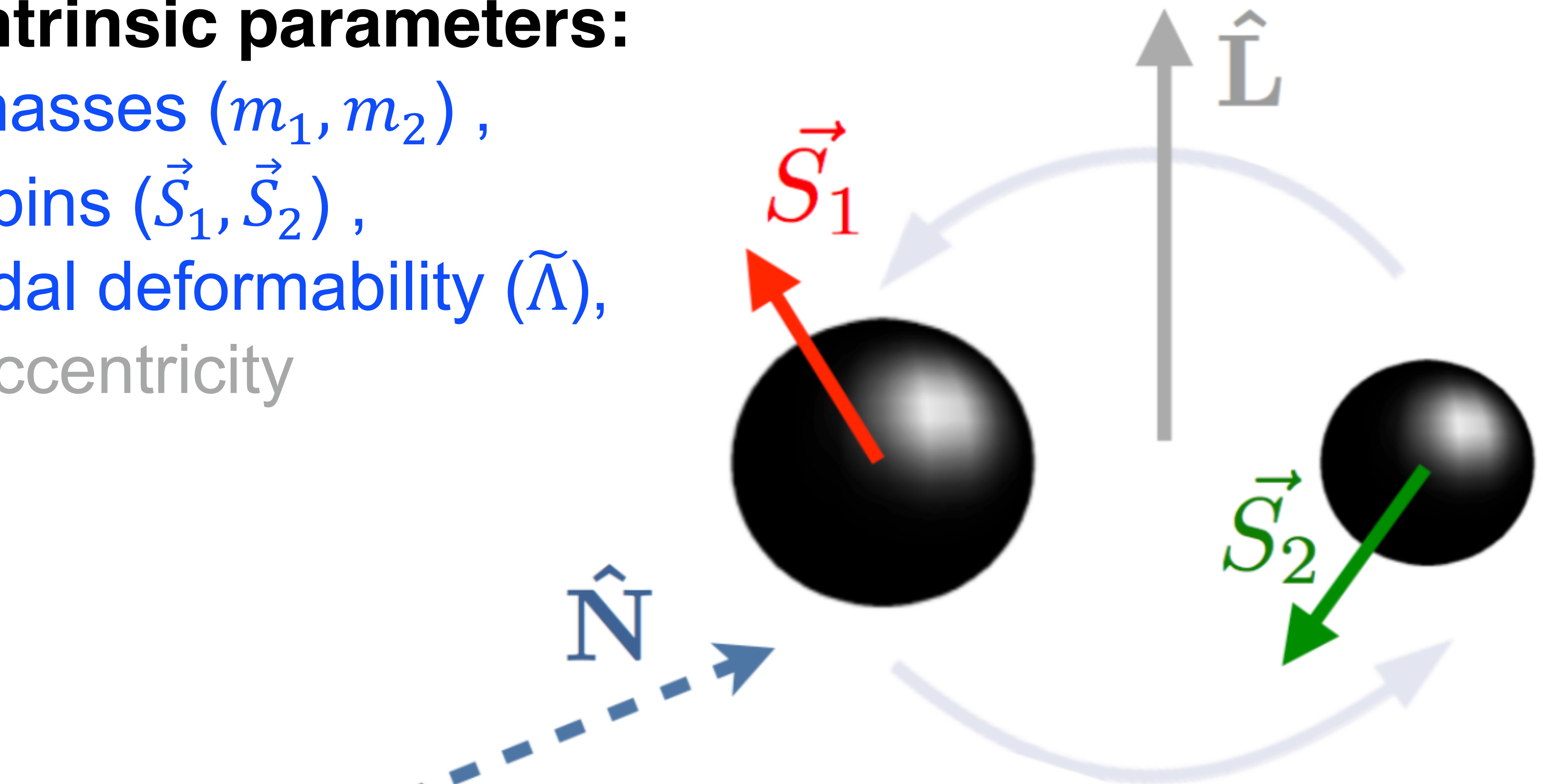
Extrinsic parameters:

time (t_c), reference phase (φ_c),
sky position (α, δ), distance (d_L),
orbital orientation (θ_{Jn}, ψ),



Credit: LIGO/Virgo

Once a signal is identified an extensive search is made against waveforms to determine its properties. Credit: Alan J. Weinstein



Spin magnitudes and orientations, eccentricity, ... tell us something about how these binaries formed

Chirp mass

What we have seen in the previous class:

$$\mathcal{M} = \frac{c^3}{G} \left(\frac{5}{96} \pi^{-8/3} f^{-11/3} \dot{f} \right)^{3/5}$$

$$h \propto \frac{\mathcal{M}^{3/5}}{r}$$

Chirp mass

What we have seen in the previous class:

$$\mathcal{M} = \frac{c^3}{G} \left(\frac{5}{96} \pi^{-8/3} f^{-11/3} \dot{f} \right)^{3/5}$$

$$h \propto \frac{\mathcal{M}^{3/5}}{r}$$

In practice we cannot ignore cosmology, and we observe a redshifted frequency:

$$\mathcal{M}(1+z) = \frac{c^3}{G} \left(\frac{5}{96} \pi^{-8/3} f_{\text{obs}}^{-11/3} \dot{f}_{\text{obs}} \right)^{3/5}$$

$$h \propto \frac{\mathcal{M}^{3/5}}{d_L}$$

Chirp mass

What we have seen in the previous class:

$$\mathcal{M} = \frac{c^3}{G} \left(\frac{5}{96} \pi^{-8/3} f^{-11/3} \dot{f} \right)^{3/5}$$

$$h \propto \frac{\mathcal{M}^{3/5}}{r}$$

In practice we cannot ignore cosmology, and we observe a redshifted frequency:

$$\mathcal{M}(1+z) = \frac{c^3}{G} \left(\frac{5}{96} \pi^{-8/3} f_{\text{obs}}^{-11/3} \dot{f}_{\text{obs}} \right)^{3/5}$$

$$h \propto \frac{\mathcal{M}^{3/5}}{d_L}$$

A distance measurement requires a cosmological model or an independent redshift measurement!

Chirp mass

What we have seen in the previous class:

$$\mathcal{M} = \frac{c^3}{G} \left(\frac{5}{96} \pi^{-8/3} f^{-11/3} \dot{f} \right)^{3/5}$$

Exercise 2

Derive the expression for the redshifted mass.

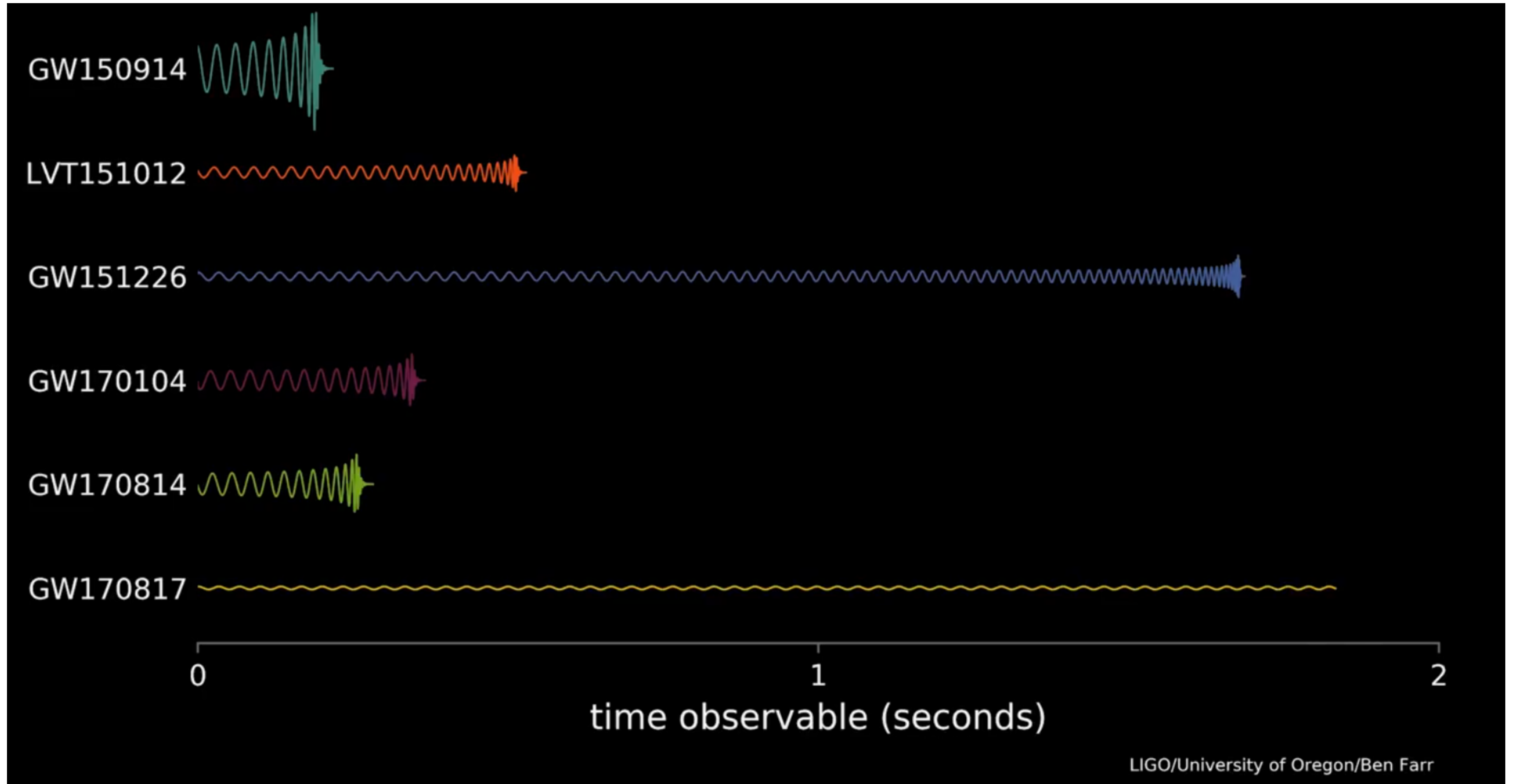
$$\mathcal{M}(1+z) = \frac{c^3}{G} \left(\frac{5}{96} \pi^{-8/3} f_{\text{obs}}^{-11/3} \dot{f}_{\text{obs}} \right)^{3/5}$$

$$h \propto \frac{\mathcal{M}^{3/5}}{d_L}$$

**A distance measurement requires a cosmological model
or an independent redshift measurement!**

Chirp mass

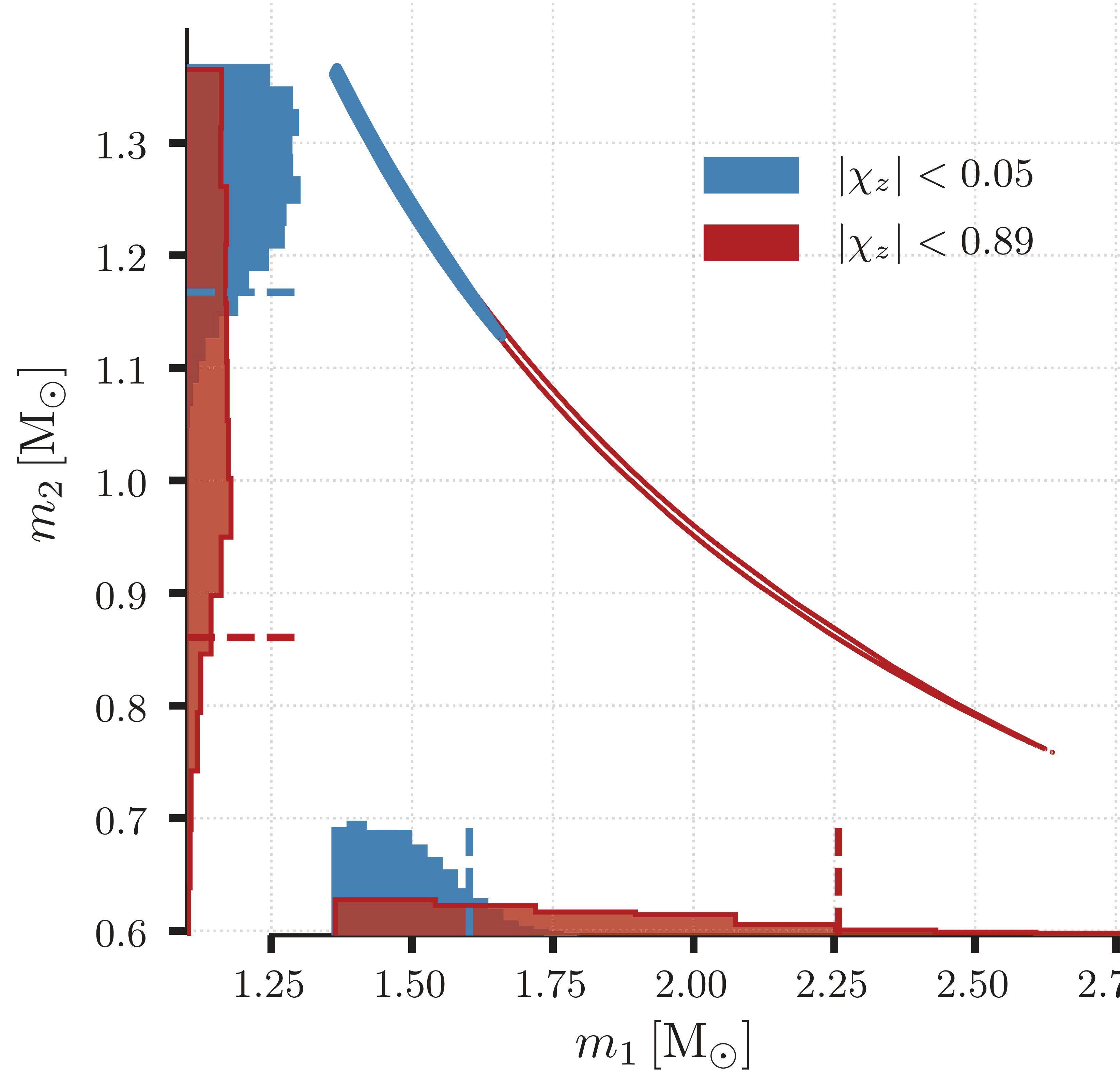
Less massive binaries are observable for more cycles



<https://www.youtube.com/watch?v=I1Ut6h6PkOw>

Chirp mass

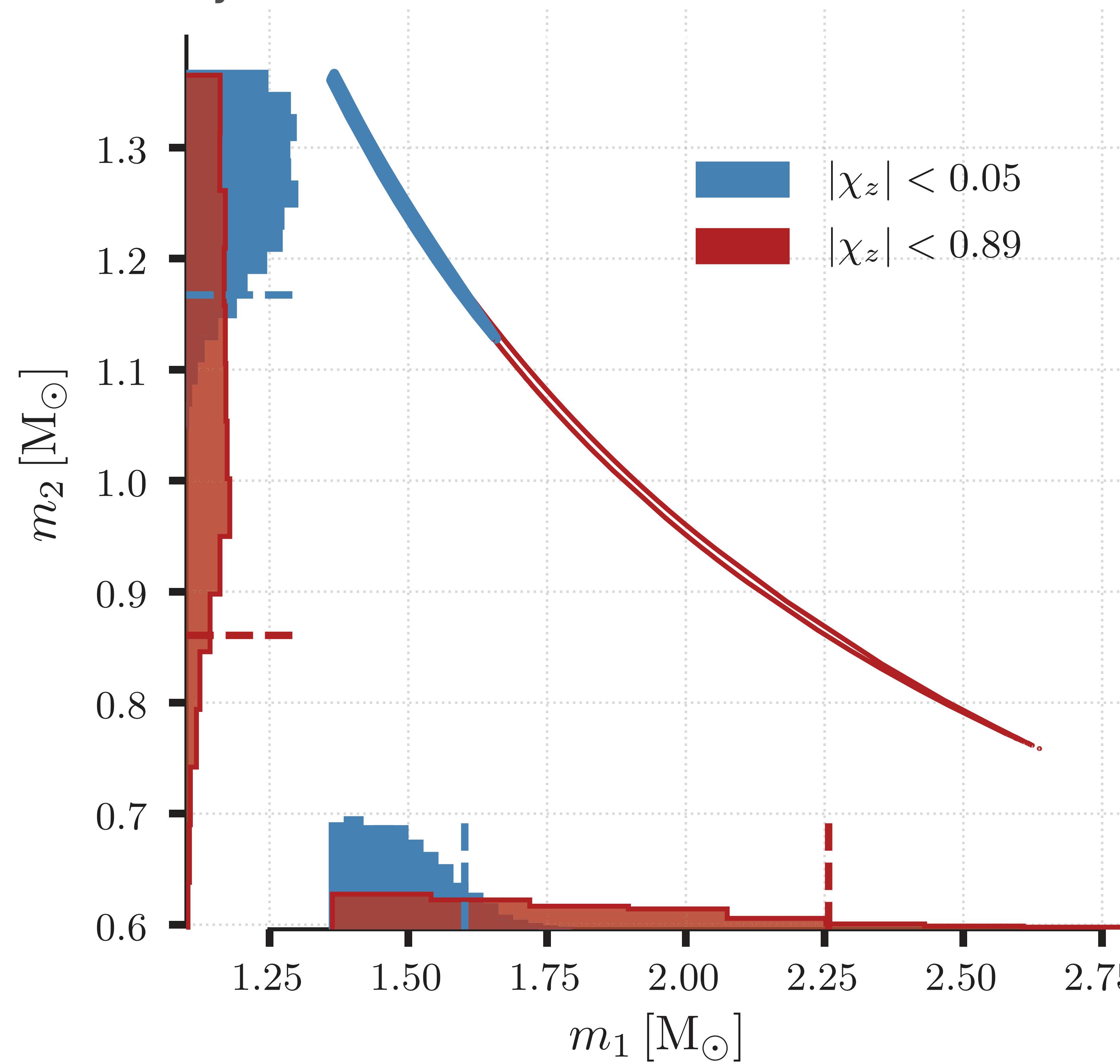
GW170817 (binary NS), discovery paper
Physical Review Letters 119, 161101 (2017)



GW170817, chirp mass determined with
a precision of 0.001 solar masses

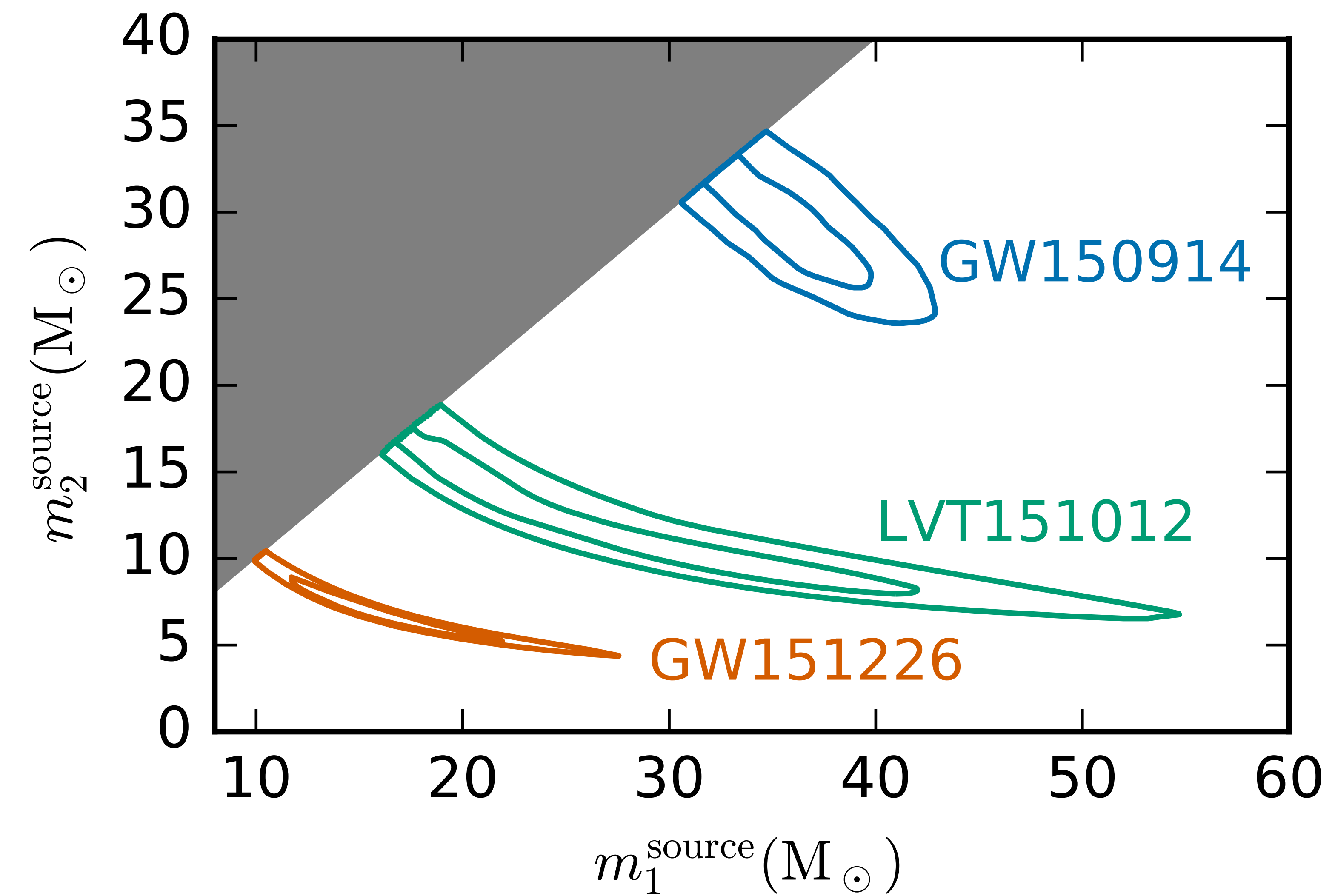
Chirp mass

GW170817 (binary NS), discovery paper
Physical Review Letters 119, 161101 (2017)



GW170817, chirp mass determined with
a precision of 0.001 solar masses

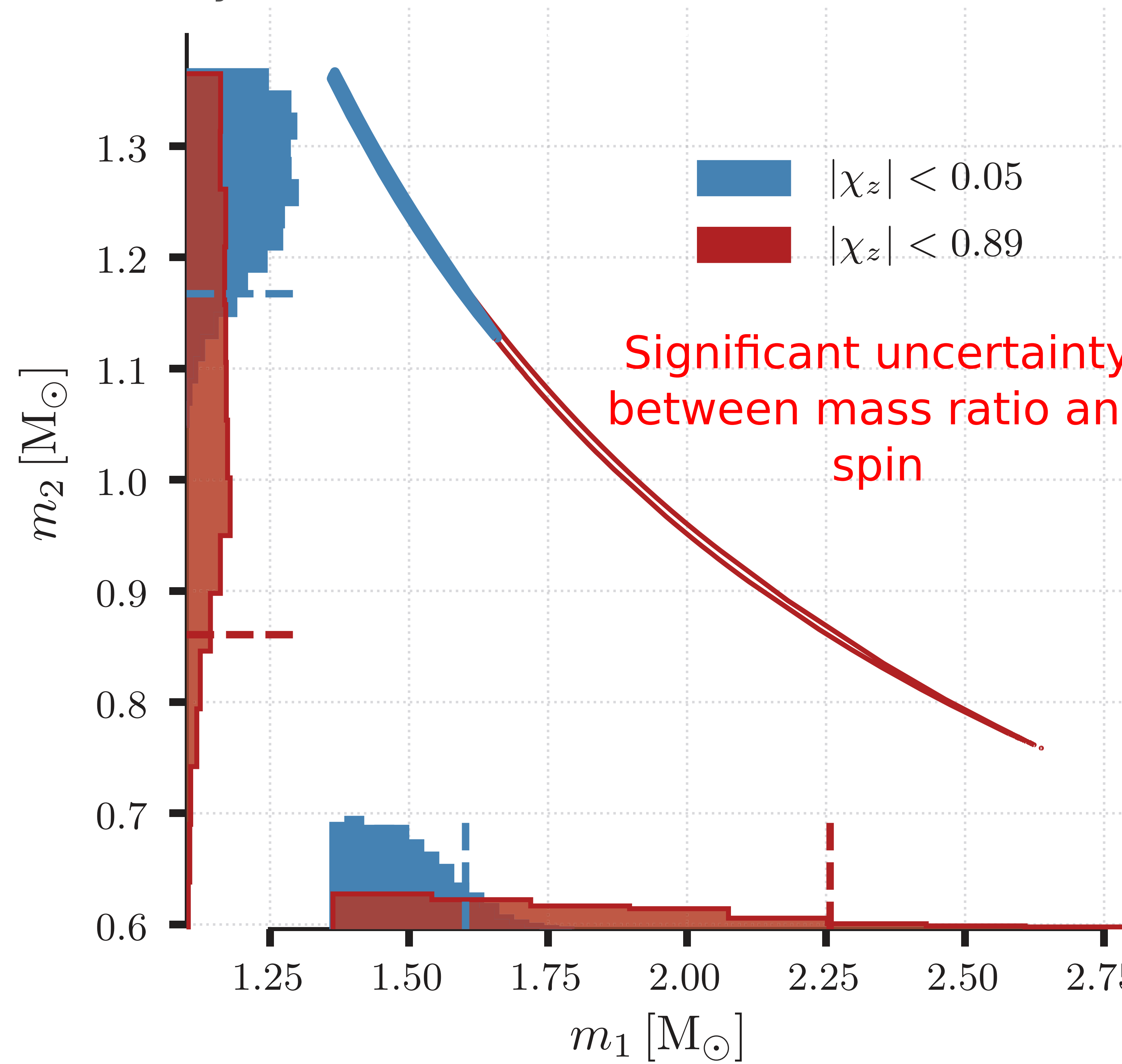
Results from LIGO's O1
Physical Review X 6, 041015 (2016)



Binary black holes have shorter
lives on band, leading to less
constrained chirp masses.

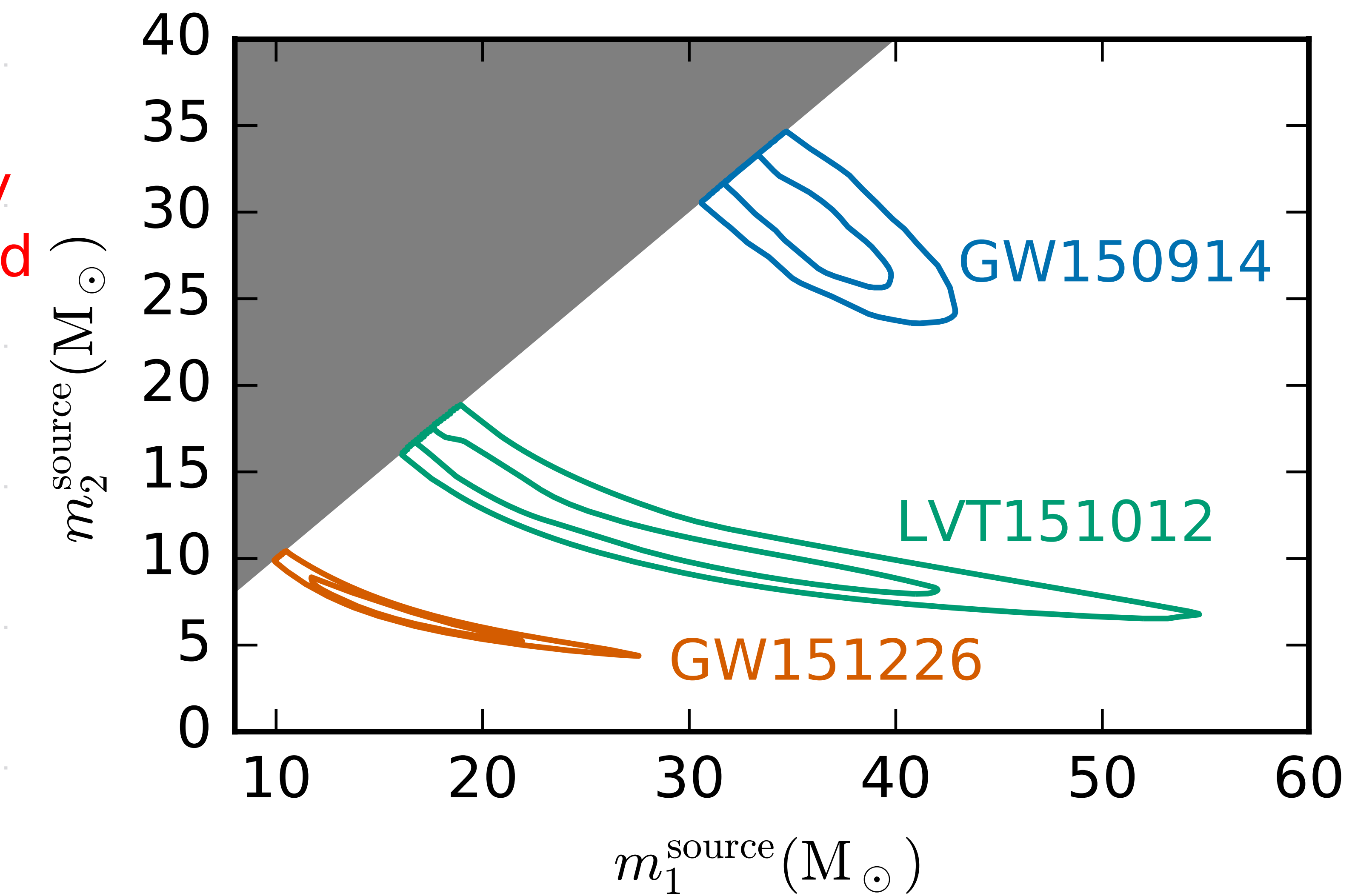
Chirp mass

GW170817 (binary NS), discovery paper
Physical Review Letters 119, 161101 (2017)



GW170817, chirp mass determined with
a precision of 0.001 solar masses

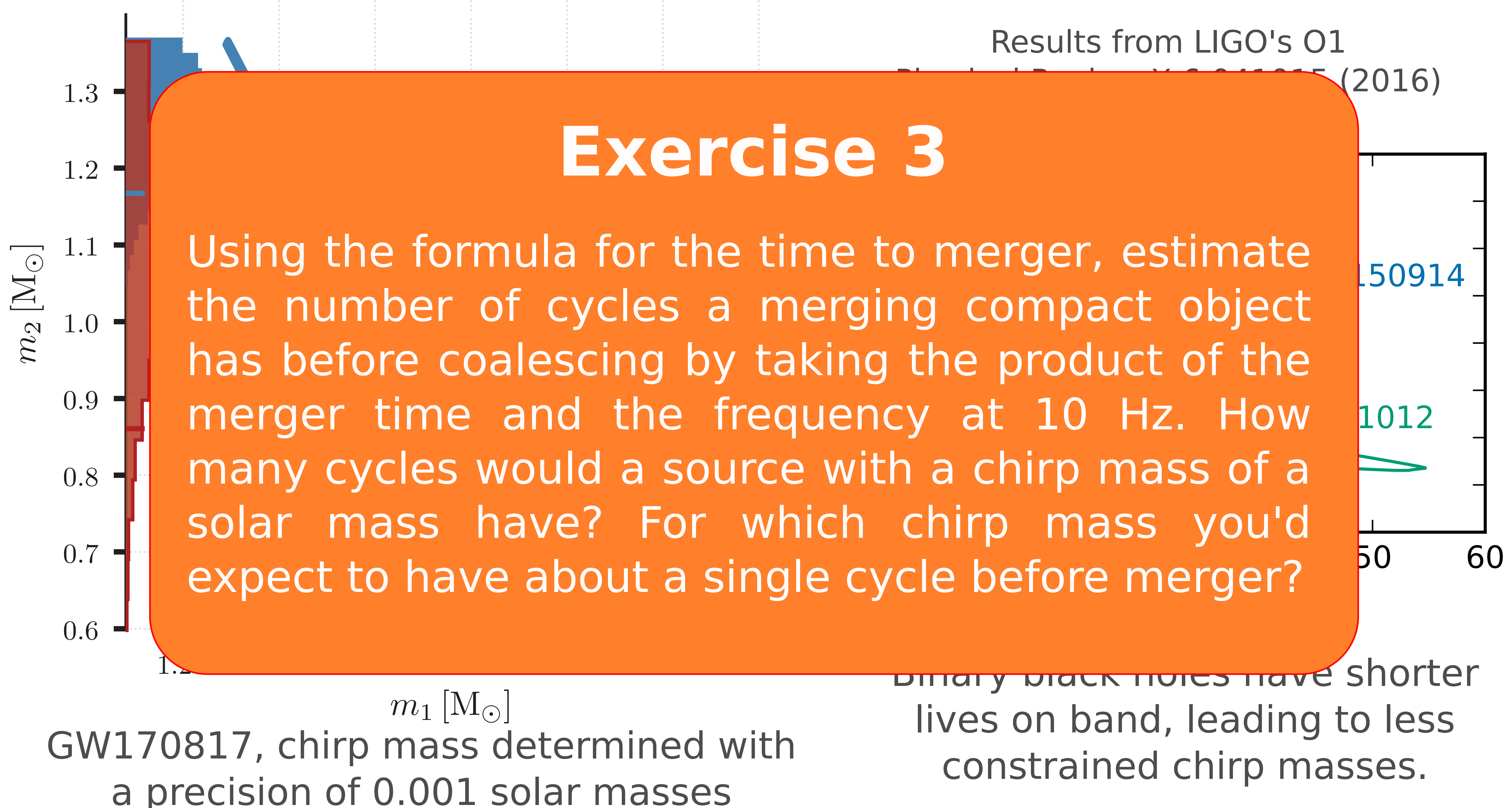
Results from LIGO's O1
Physical Review X 6, 041015 (2016)



Binary black holes have shorter
lives on band, leading to less
constrained chirp masses.

Chirp mass

GW170817 (binary NS), discovery paper
Physical Review Letters 119, 161101 (2017)



Mass ratio and spin

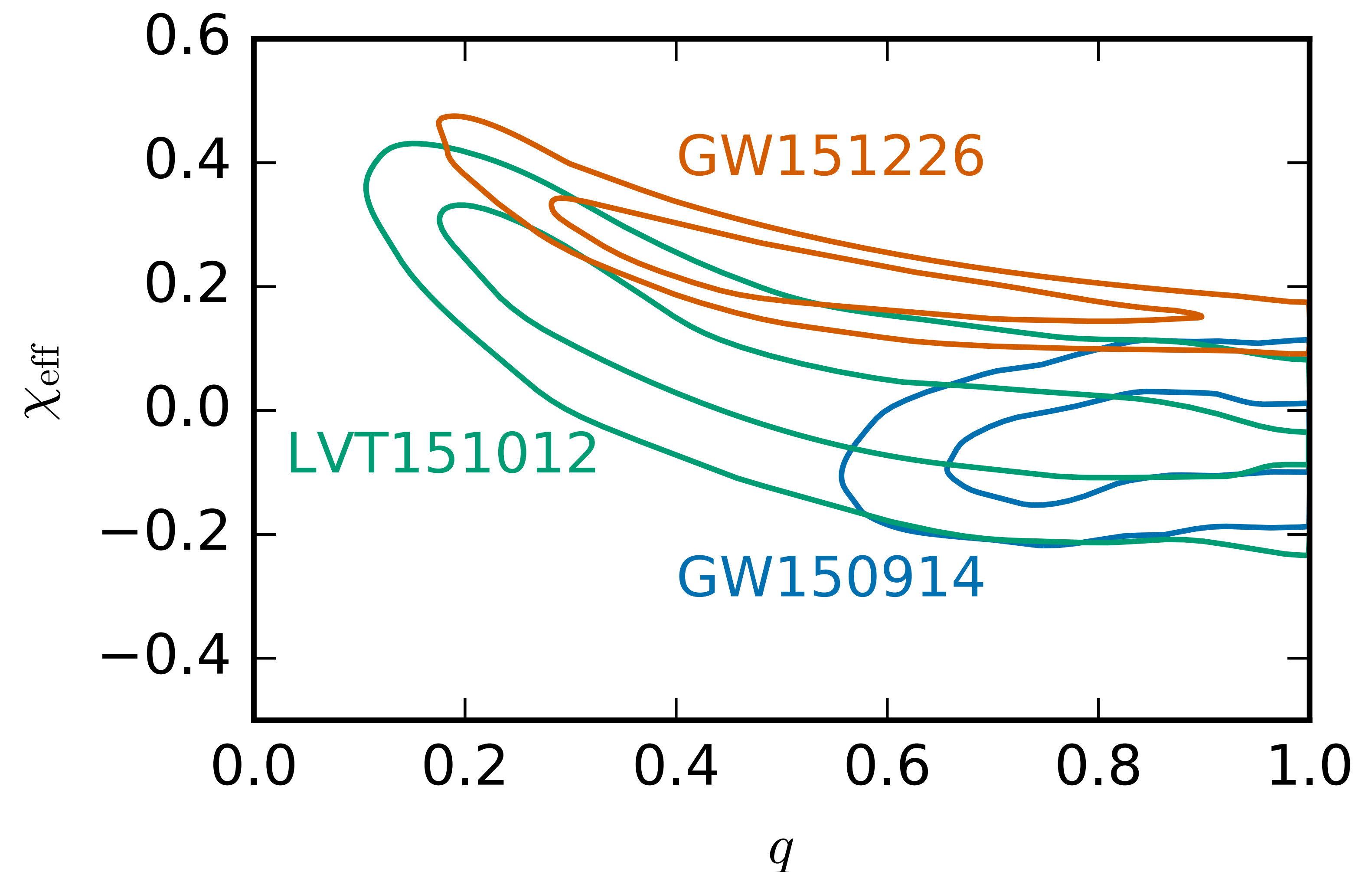
After the chirp mass, the best constrained quantities are usually the **mass ratio** and the **effective spin**:

$$q = m_2/m_1$$

$$\chi_{\text{eff}} = \frac{m_1 \chi_1 + m_2 \chi_2}{m_1 + m_2}$$

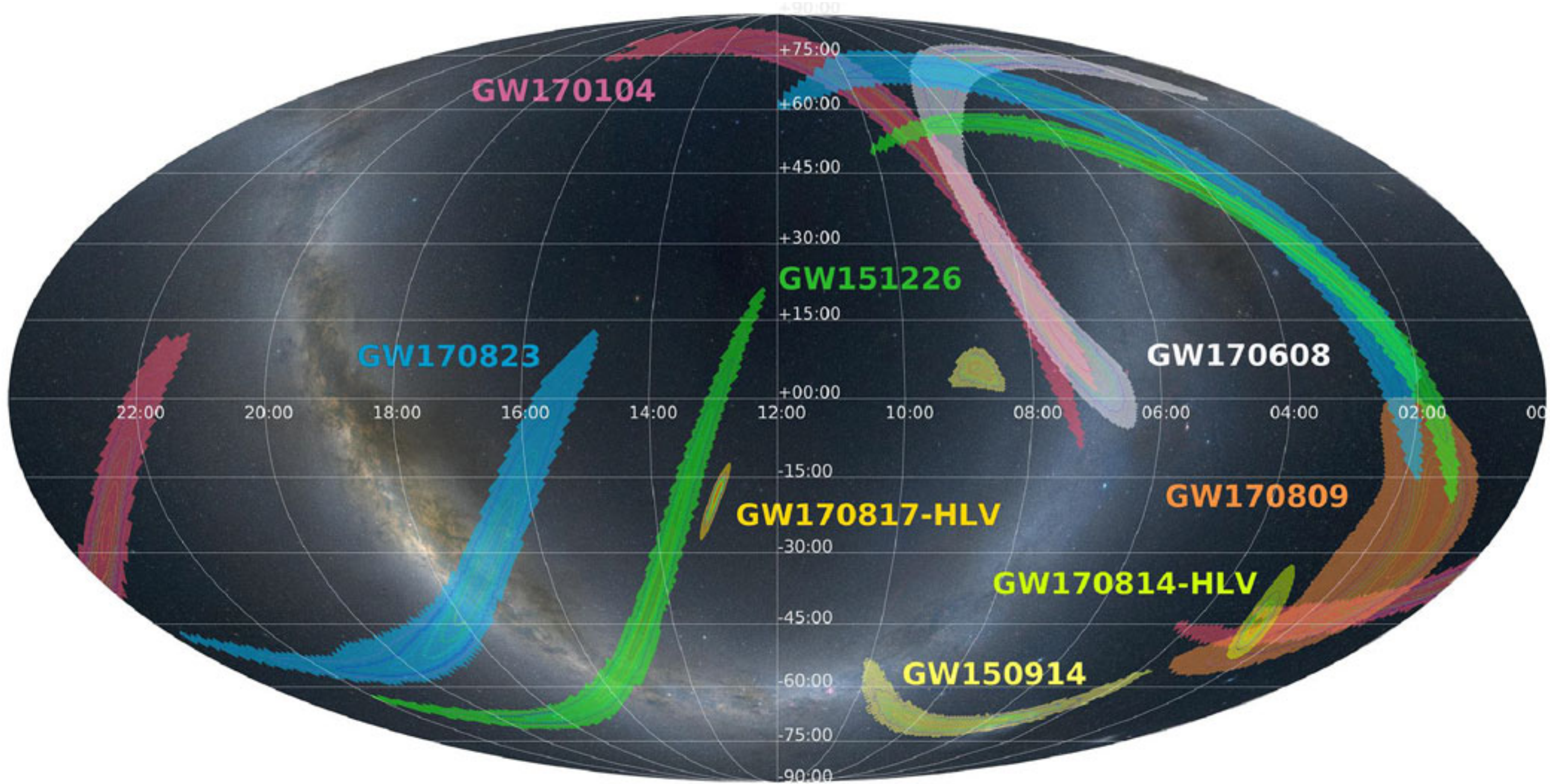
Where the chi give the components of the spin aligned with the orbital plane.

These two parameters have a degenerate effect on the waveform, though this degeneracy can be broken with sufficiently accurate observations.

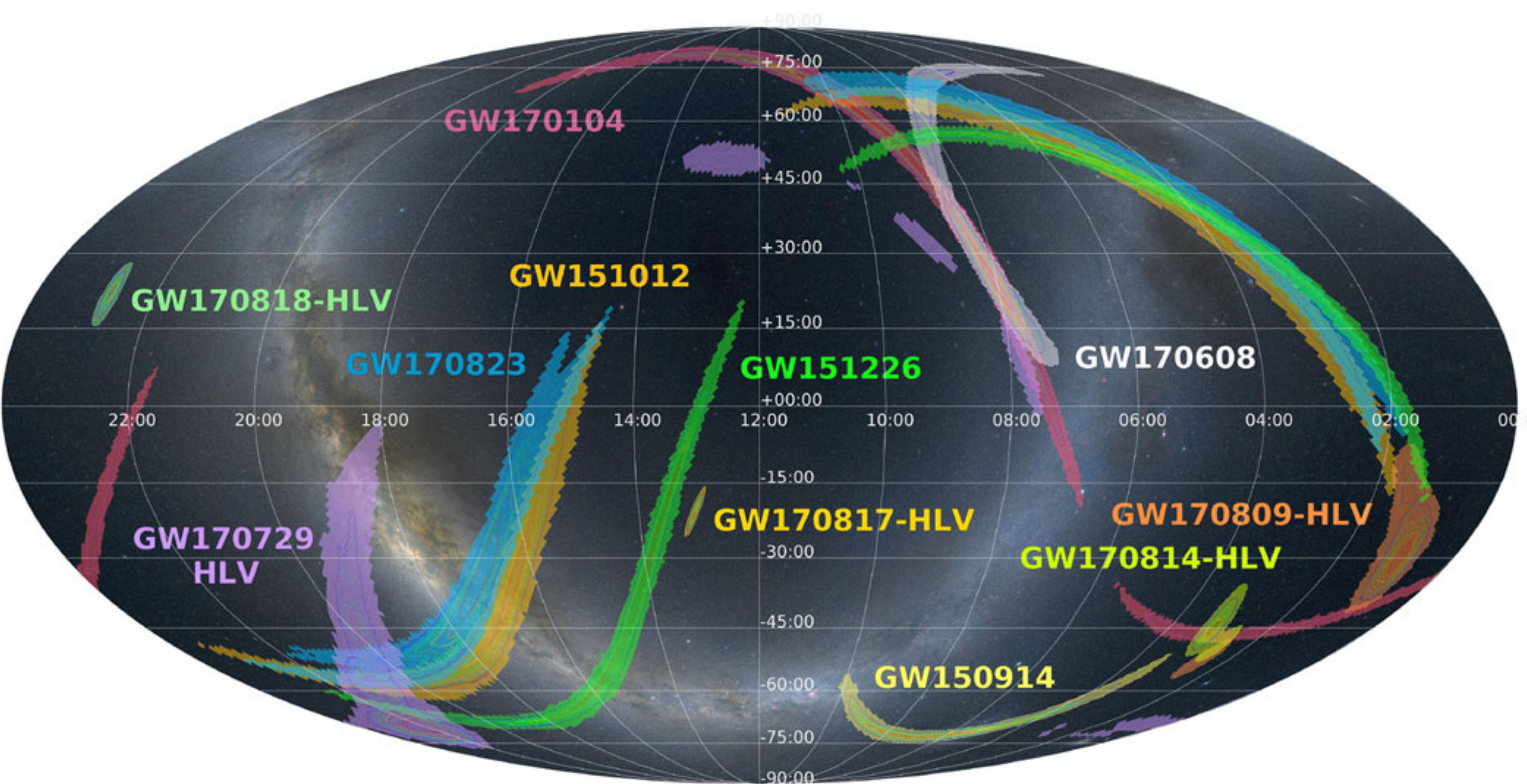


Results from LIGO's O1
Physical Review X 6,041015 (2016)

Localization

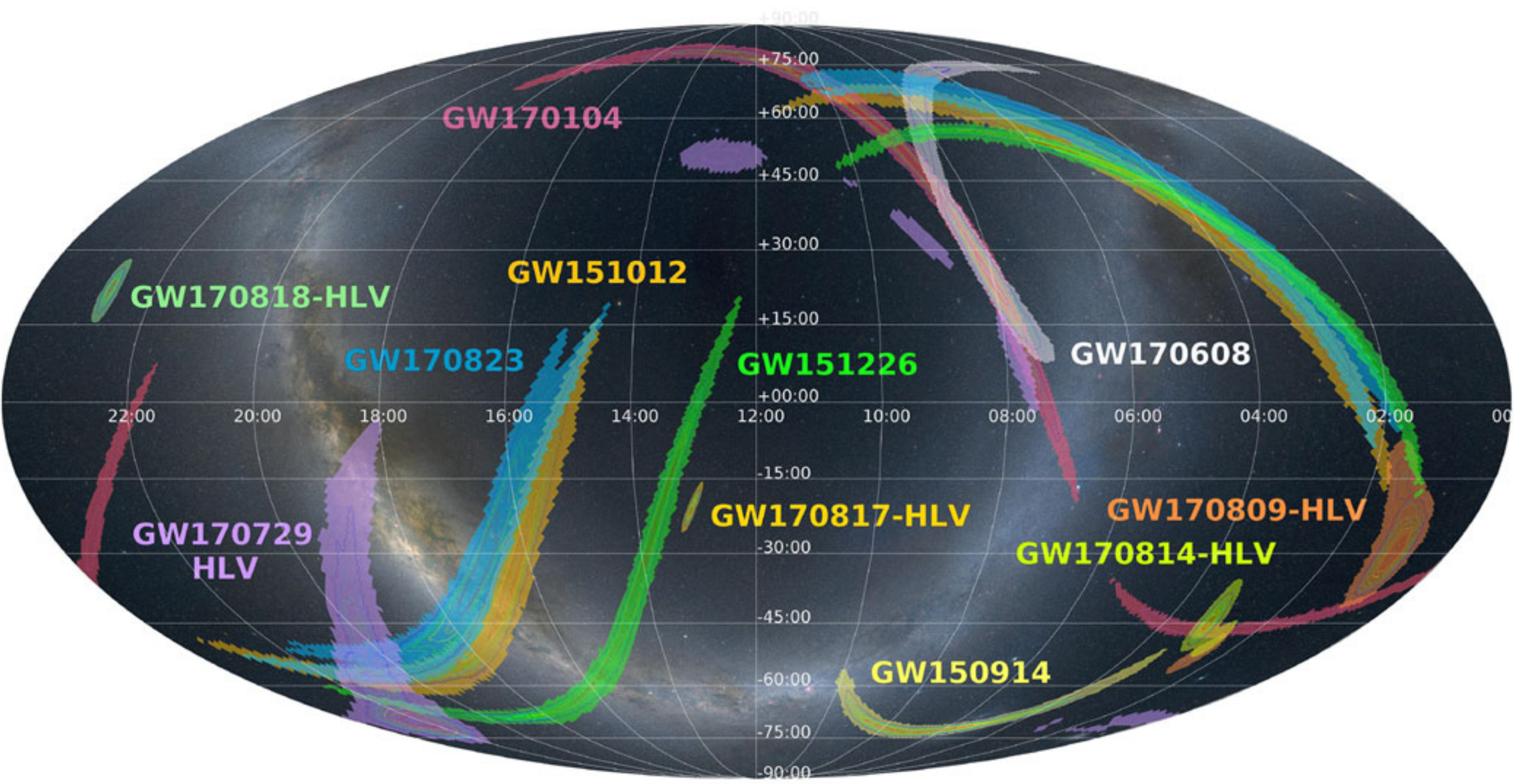
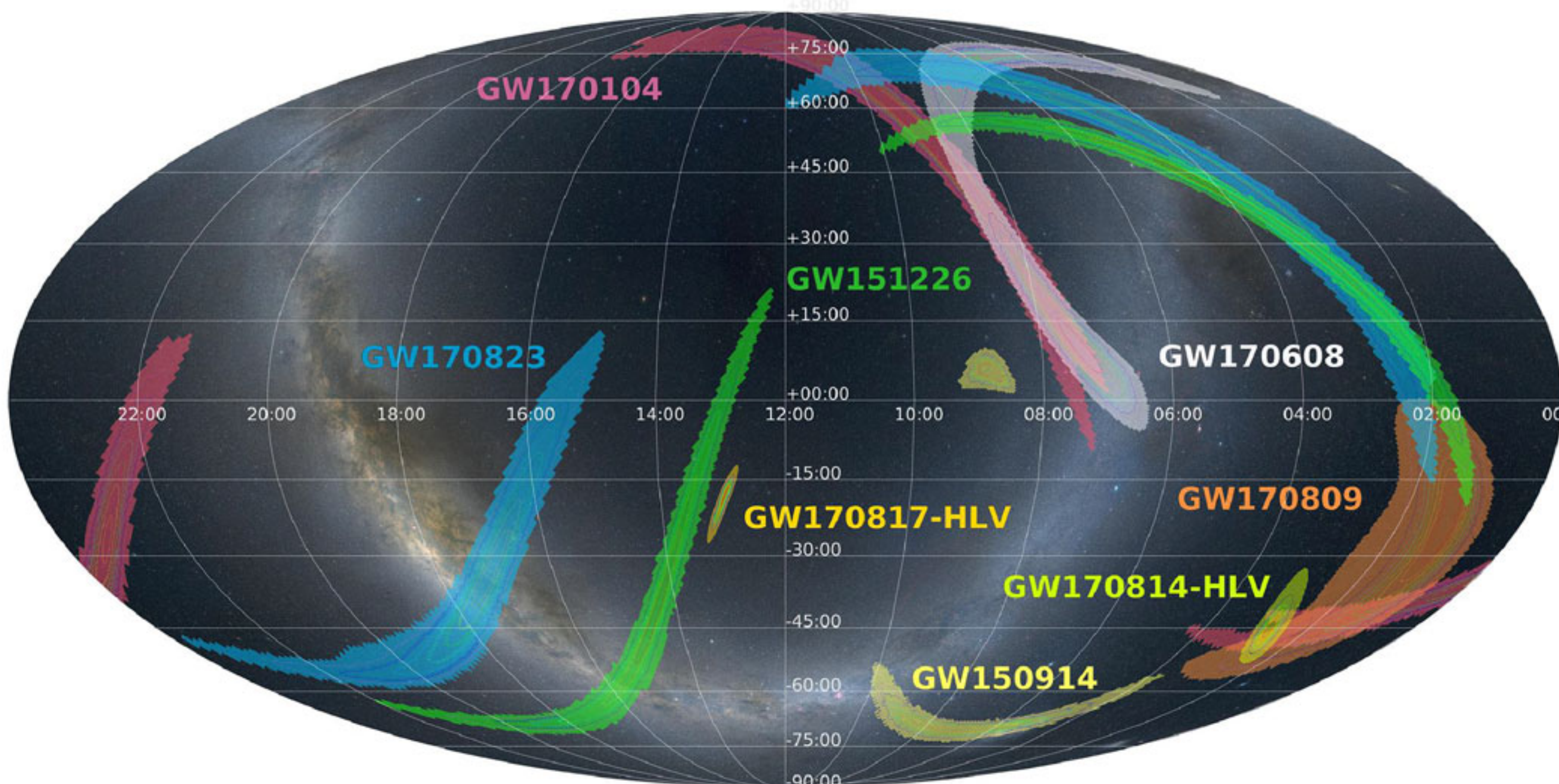


Localization of sources comes mostly from triangulation. Except for a couple of sources, uncertainty in location is more than 100 square degrees.



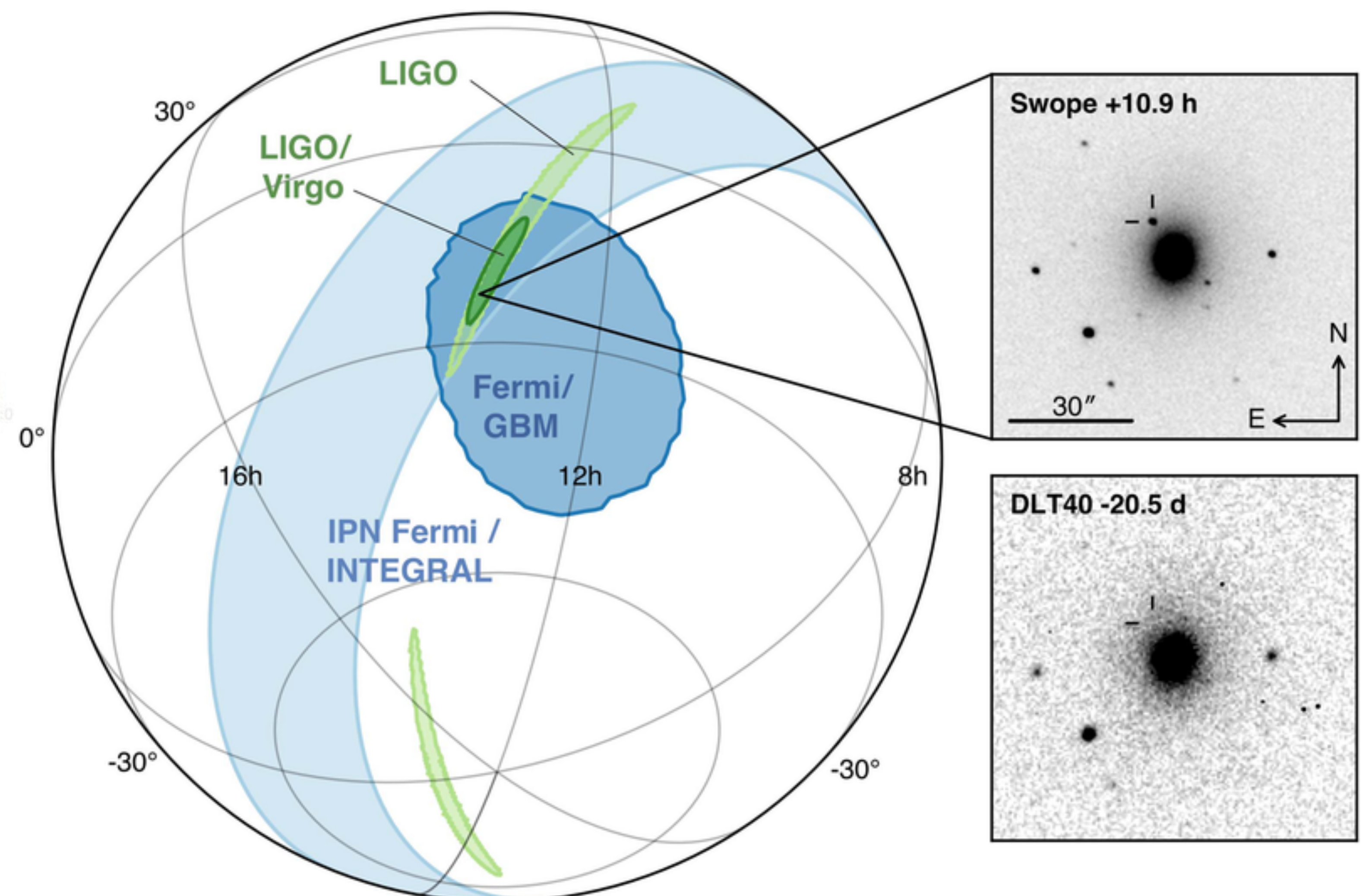
Prospects for localization of sources
Living Reviews in Relativity volume 21,
Article number: 3 (2018)

Localization



Prospects for localization of sources
Living Reviews in Relativity volume 21,
Article number: 3 (2018)

Localization of sources comes mostly from triangulation. Except for a couple of sources, uncertainty in location is more than 100 square degrees.



credit: LIGO-Virgo collaboration

And from all this, catalogues!

B. P. ABBOTT *et al.*

PHYS. REV. X **9**, 031040 (2019)

TABLE III. Selected source parameters of the 11 confident detections. We report median values with 90% credible intervals that include statistical errors and systematic errors from averaging the results of two waveform models for BBHs. For GW170817, credible intervals and statistical errors are shown for IMRPhenomPv2NRT with a low spin prior, while the sky area is computed from TaylorF2 samples. The redshift for NGC 4993 from Ref. [94] and its associated uncertainties are used to calculate source-frame masses for GW170817. For BBH events, the redshift is calculated from the luminosity distance and assumed cosmology as discussed in Appendix B. The columns show source-frame component masses m_i and chirp mass \mathcal{M} , dimensionless effective aligned spin χ_{eff} , final source-frame mass M_f , final spin a_f , radiated energy E_{rad} , peak luminosity l_{peak} , luminosity distance d_L , redshift z , and sky localization $\Delta\Omega$. The sky localization is the area of the 90% credible region. For GW170817, we give conservative bounds on parameters of the final remnant discussed in Sec. V E.

Event	m_1/M_\odot	m_2/M_\odot	\mathcal{M}/M_\odot	χ_{eff}	M_f/M_\odot	a_f	$E_{\text{rad}}/(M_\odot c^2)$	$l_{\text{peak}}/(\text{erg s}^{-1})$	d_L/Mpc	z	$\Delta\Omega/\text{deg}^2$
GW150914	$35.6^{+4.7}_{-3.1}$	$30.6^{+3.0}_{-4.4}$	$28.6^{+1.7}_{-1.5}$	$-0.01^{+0.12}_{-0.13}$	$63.1^{+3.4}_{-3.0}$	$0.69^{+0.05}_{-0.04}$	$3.1^{+0.4}_{-0.4}$	$3.6^{+0.4}_{-0.4} \times 10^{56}$	440^{+150}_{-170}	$0.09^{+0.03}_{-0.03}$	182
GW151012	$23.2^{+14.9}_{-5.5}$	$13.6^{+4.1}_{-4.8}$	$15.2^{+2.1}_{-1.2}$	$0.05^{+0.31}_{-0.20}$	$35.6^{+10.8}_{-3.8}$	$0.67^{+0.13}_{-0.11}$	$1.6^{+0.6}_{-0.5}$	$3.2^{+0.8}_{-1.7} \times 10^{56}$	1080^{+550}_{-490}	$0.21^{+0.09}_{-0.09}$	1523
GW151226	$13.7^{+8.8}_{-3.2}$	$7.7^{+2.2}_{-2.5}$	$8.9^{+0.3}_{-0.3}$	$0.18^{+0.20}_{-0.12}$	$20.5^{+6.4}_{-1.5}$	$0.74^{+0.07}_{-0.05}$	$1.0^{+0.1}_{-0.2}$	$3.4^{+0.7}_{-1.7} \times 10^{56}$	450^{+180}_{-190}	$0.09^{+0.04}_{-0.04}$	1033
GW170104	$30.8^{+7.3}_{-5.6}$	$20.0^{+4.9}_{-4.6}$	$21.4^{+2.2}_{-1.8}$	$-0.04^{+0.17}_{-0.21}$	$48.9^{+5.1}_{-4.0}$	$0.66^{+0.08}_{-0.11}$	$2.2^{+0.5}_{-0.5}$	$3.3^{+0.6}_{-1.0} \times 10^{56}$	990^{+440}_{-430}	$0.20^{+0.08}_{-0.08}$	921
GW170608	$11.0^{+5.5}_{-1.7}$	$7.6^{+1.4}_{-2.2}$	$7.9^{+0.2}_{-0.2}$	$0.03^{+0.19}_{-0.07}$	$17.8^{+3.4}_{-0.7}$	$0.69^{+0.04}_{-0.04}$	$0.9^{+0.0}_{-0.1}$	$3.5^{+0.4}_{-1.3} \times 10^{56}$	320^{+120}_{-110}	$0.07^{+0.02}_{-0.02}$	392
GW170729	$50.2^{+16.2}_{-10.2}$	$34.0^{+9.1}_{-10.1}$	$35.4^{+6.5}_{-4.8}$	$0.37^{+0.21}_{-0.25}$	$79.5^{+14.7}_{-10.2}$	$0.81^{+0.07}_{-0.13}$	$4.8^{+1.7}_{-1.7}$	$4.2^{+0.9}_{-1.5} \times 10^{56}$	2840^{+1400}_{-1360}	$0.49^{+0.19}_{-0.21}$	1041
GW170809	$35.0^{+8.3}_{-5.9}$	$23.8^{+5.1}_{-5.2}$	$24.9^{+2.1}_{-1.7}$	$0.08^{+0.17}_{-0.17}$	$56.3^{+5.2}_{-3.8}$	$0.70^{+0.08}_{-0.09}$	$2.7^{+0.6}_{-0.6}$	$3.5^{+0.6}_{-0.9} \times 10^{56}$	1030^{+320}_{-390}	$0.20^{+0.05}_{-0.07}$	308
GW170814	$30.6^{+5.6}_{-3.0}$	$25.2^{+2.8}_{-4.0}$	$24.1^{+1.4}_{-1.1}$	$0.07^{+0.12}_{-0.12}$	$53.2^{+3.2}_{-2.4}$	$0.72^{+0.07}_{-0.05}$	$2.7^{+0.4}_{-0.3}$	$3.7^{+0.4}_{-0.5} \times 10^{56}$	600^{+150}_{-220}	$0.12^{+0.03}_{-0.04}$	87
GW170817	$1.46^{+0.12}_{-0.10}$	$1.27^{+0.09}_{-0.09}$	$1.186^{+0.001}_{-0.001}$	$0.00^{+0.02}_{-0.01}$	≤ 2.8	≤ 0.89	≥ 0.04	$\geq 0.1 \times 10^{56}$	40^{+7}_{-15}	$0.01^{+0.00}_{-0.00}$	16
GW170818	$35.4^{+7.5}_{-4.7}$	$26.7^{+4.3}_{-5.2}$	$26.5^{+2.1}_{-1.7}$	$-0.09^{+0.18}_{-0.21}$	$59.4^{+4.9}_{-3.8}$	$0.67^{+0.07}_{-0.08}$	$2.7^{+0.5}_{-0.5}$	$3.4^{+0.5}_{-0.7} \times 10^{56}$	1060^{+420}_{-380}	$0.21^{+0.07}_{-0.07}$	39
GW170823	$39.5^{+11.2}_{-6.7}$	$29.0^{+6.7}_{-7.8}$	$29.2^{+4.6}_{-3.6}$	$0.09^{+0.22}_{-0.26}$	$65.4^{+10.1}_{-7.4}$	$0.72^{+0.09}_{-0.12}$	$3.3^{+1.0}_{-0.9}$	$3.6^{+0.7}_{-1.1} \times 10^{56}$	1940^{+970}_{-900}	$0.35^{+0.15}_{-0.15}$	1666

Want to know more?

 https://astro-gr.org/online-course-gravitational-waves/

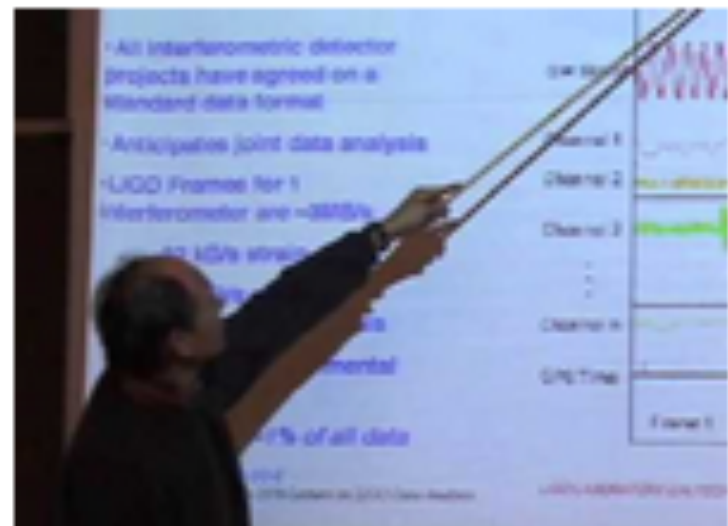
Astro-GR

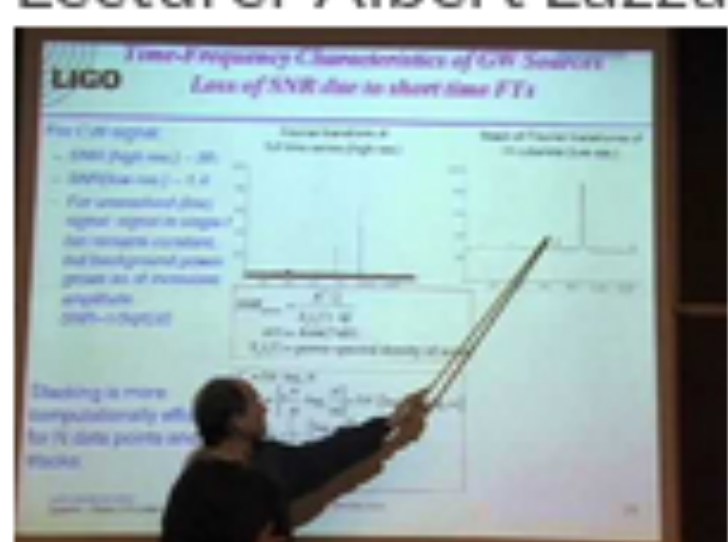
Home Me Contact Focus About Team Grav. Wave Course GW Notes Stellar Collisions ▾ Workshops ▾ Pap

Pygmalion ▾ OpenBSD ▾ WP ▾ Life ▾ Comments et al ▾

8 – LIGO Data Analysis – slides, assignments and solutions

1. The context: LIGO-I noise curve and anticipated signal strengths
2. LIGO data attributes
3. Some signal processing theory and methods
4. Optimal filtering for parametrizable waveforms
5. Stochastic background searches
6. Hypothesis testing: maximum likelihood; Baysean statistics; false alarm probability compared with detection probability
7. Searching for (transient) bursts of GW's
8. Analysis of data from a network of detectors

Lecturer Albert Lazzarini: "LIGO Data Analysis (1/2)"


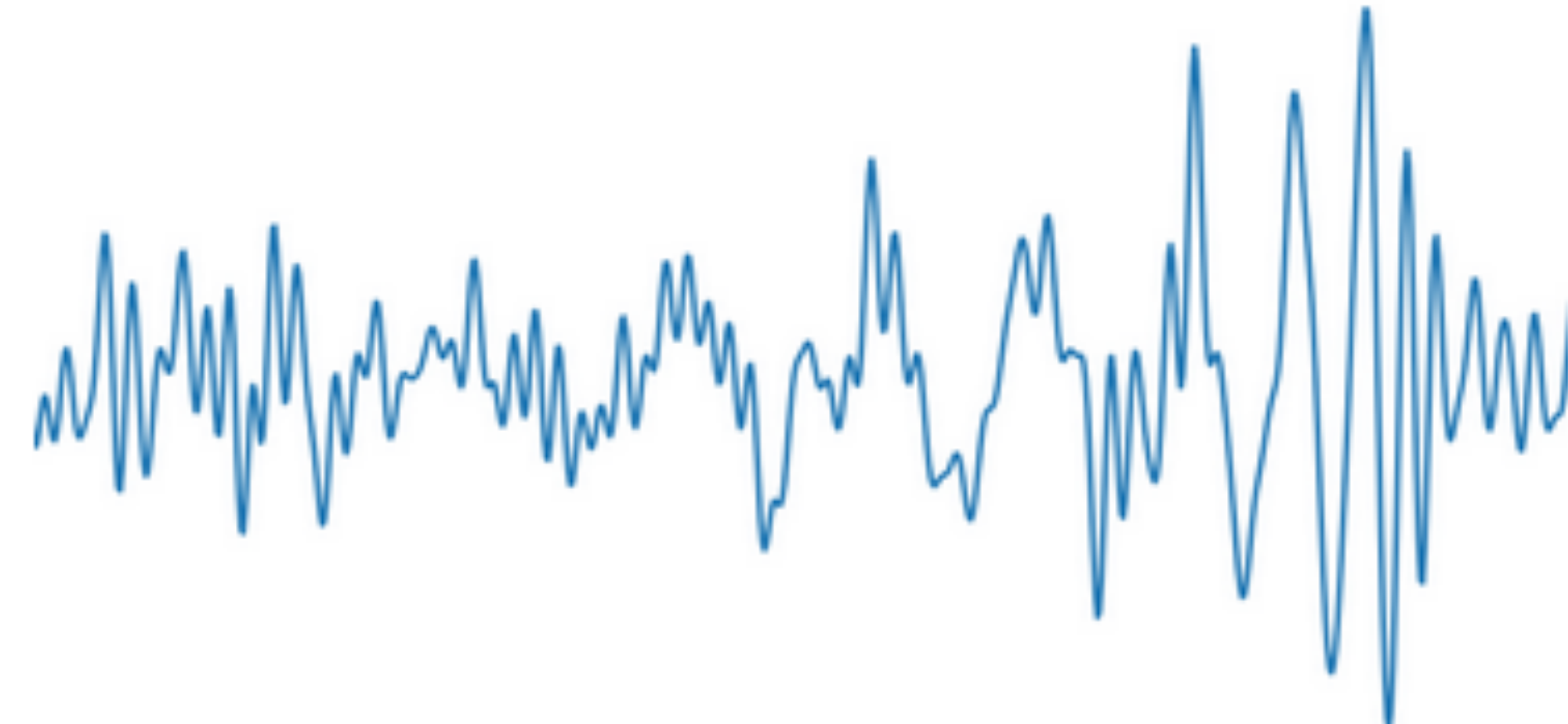
Lecturer Albert Lazzarini: "LIGO Data Analysis (2/2)"


Astro-GR course has some lectures on LIGO data analysis.
But better to use more up to date info!

Want to know more?



<https://www.gw-openscience.org/s/workshop3/>



LIGO - Virgo Collaboration GW Open Data Workshop #3

May 26 - 28, 2020

GW ODW #3

Location

Registration

Program

GWOSC

Gravitational-Wave Open Data Workshop #3

Advanced LIGO and Advanced Virgo are now observing the gravitational-wave sky with unprecedented sensitivity. To date, there have been over 50 potential gravitational-wave transients observed, and planned detector upgrades are likely to accelerate the pace of discovery in the coming years. This new window on the universe is providing insights on a range of topics, including compact body populations, cosmology, and fundamental physics.

LIGO and Virgo strain data from past observation runs and data snippets around discoveries are made publicly available at gw-openscience.org, along with associated software libraries. The LIGO and Virgo collaborations are hosting an Open Data Workshop to facilitate working with these data products. This workshop is the third edition of a [series](#) that began in 2018. It is intended for scientists and students who wish to learn about using gravitational-wave data and software in order to conduct research of their own. The workshop will provide a mixture of lecture style presentations and hands-on programming exercises, using publicly available gravitational-wave data and specialized software tools.

Presentations from open data workshops of the LVC are available online. [workshop1](#) and [workshop2](#) available also!

Want to know more?

Living Rev. Relativity, **12**, (2009), 2
<http://www.livingreviews.org/lrr-2009-2>



Physics, Astrophysics and Cosmology with Gravitational Waves

B.S. Sathyaprakash

School of Physics and Astronomy, Cardiff University,
Cardiff, U.K.
email: B.Sathyaprakash@astro.cf.ac.uk

Bernard F. Schutz

School of Physics and Astronomy, Cardiff University,
Cardiff, U.K.
and
Max Planck Institute for Gravitational Physics
(Albert Einstein Institute)
Potsdam-Golm, Germany
email: Bernard.Schutz@aei.mpg.de

Really a good review for both parts of
today's lecture.

Living Reviews in Relativity

ISSN 1433-8351

Accepted on 29 January 2009
Published on 4 March 2009

Abstract

Gravitational wave detectors are already operating at interesting sensitivity levels, and they have an upgrade path that should result in secure detections by 2014. We review the physics of gravitational waves, how they interact with detectors (bars and interferometers), and how these detectors operate. We study the most likely sources of gravitational waves and review the data analysis methods that are used to extract their signals from detector noise. Then we consider the consequences of gravitational wave detections and observations for physics, astrophysics, and cosmology.

Want to know more?

OPEN ACCESS

IOP Publishing

Classical and Quantum Gravity

Class. Quantum Grav. **37** (2020) 055002 (54pp)

<https://doi.org/10.1088/1361-6382/ab685e>

A guide to LIGO–Virgo detector noise and extraction of transient gravitational-wave signals

Up to date overview of the methods being used for signal processing.